Fine-grained rims surrounding chondrules in the Tagish Lake carbonaceous chondrite: Verification of their formation through parent-body processes

Takayama, Akiko

(Degree)
博士（理学）

(Date of Degree)
2012-09-25

(Date of Publication)
2013-04-02

(Resource Type)
doctoral thesis

(Report Number)
甲5644

(URL)
https://hdl.handle.net/20.500.14094/D1005644

博士論文

Fine-grained rims surrounding chondrules in the Tagish Lake carbonaceous chondrite: Verification of their formation through parent-body processes

(Tagish Lake 炭素質隕石のコンドリュールを取り囲む細粒リム：
母天体上のプロセスによる形成の検証)

平成２４年７月

神戸大学大学院理学研究科

髙山　亜紀子

Akiko TAKAYAMA

博士論文

Fine-grained rims surrounding chondrules in the Tagish Lake carbonaceous chondrite: Verification of their formation through parent-body processes

(Tagish Lake 炭素質隕石のコンドリュールを取り囲む細粒リム：母天体上のプロセスによる形成の検証)

平成 24 年 7 月

神戸大学大学院理学研究科

髙山　亜紀子

Akiko TAKAYAMA

ABSTRACT

Chapter 1: Introduction. Planetary materials are products formed through the evolution process of the solar system, thus they have information about the formation history of it. However, on the differenciated bodies such as planets, elements in materials have been equilibrated and their original characteristics have been overprinted. Thus we focus on uniquilibrated materials from smaller bodies (asteroids): meteorites, interplanetary dust particles (IDPs) and micrometeorites (MMs). Hydration of minerals is thought to have occurred on the primitive planetesimals, thus hydrous planetary materials are important key to uncover the early processes of the solar system. Nearly half of IDPs and MMs are hydrous, although hydrous meteorites are significantly low in abundance. Tagish Lake carbonaceous chondrite is thoght to be the first sample from D type asteroids, which are representative hydrous asteroids. This meteorite consists of two major lithologies: carbonate-poor and carbonate-rich. One of the remarkable characteristics of this meteorite is the general presence of fine-grained chondrule rims. Fine-grained rims are commonly observed in other meteorites such as CM, CV and ordinary chondrites, although the formation mechanism of the rims has been controvertial. Most commonly recognized model is that rims were formed by accretion of the dusts in the early solar nebula (e.g. Metzler et al., 1992). Another model is that rims were formed by a series of parent body processes (e.g. Tomeoka and Tanimura, 2000). Regarding the fine-grained rims in Tagish Lake, completely different formation processes have been proposed for each of the two lithologies. Nakamura et al. (2003) proposed that the rims in the carbonate-rich lithology were formed on the parent body (or bodies); though Greshake et al. (2005) proposed that the rims in the carbonate-poor

lithology were formed by accretion of dusts in the nebula. Nakamura et al. (2003) stated that there is a possibility that the origin of the rim in the carbonate-rich lithology have a link to the carbonate-poor lithology. However, no study on the carbonate-poor lithology which considers that possibility has been done.

In this paper, I present the results of detailed petrographic and mineralogical investigation of the carbonate-poor lithology of the Tagish Lake meteorite. My goal in this study is to find any evidence indicating the processes and conditions of rim formation, to determine which of the above or other models of rim formation most consistently explains the mineralogical and petrographic characteristics of the rims and other components, and to elucidate the formation history of the Tagish Lake carbonate-poor lithology.

Chapter 2: Samples and methods. Two polished thin sections of Tagish Lake were studied using scanning electron microscope (SEM) and electron probe microanalyser (EPMA). For calculating the modal abundances of the coarse components, pseudomorphs and minerals, they were colored on BSE images and pixels of them were counted on Adobe Photoshop Software.

Chapter 3: Results. The carbonate-poor lithology of the Tagish Lake carbonaceous chondrite consists of a dominant matrix (84.1 vol.%) and 87 chondrules (11.1 vol.%), 2 Ca-Al-rich inclusions (CAIs) (0.4 vol.%), and 14 forsterite aggregates (2.1 vol.%). Matrix contains abundant pores and exhibit an uneven surface. The matrix mainly consists of fine-grained phyllosilicates with minor amount of Fe-Mg carbonate, magnetite, forsteritic olivine, Ca carbonate, and Fe-(Ni) sulfides.

The chondrules consist of extremely Fe-poor olivine (Fo) and pyroxene (En). Most forsterite phenocrysts show little evidence of alteration, whereas most enstatite

phenocrysts were partly or totally replaced by Mg-rich phyllosilicates. Mesostases were completely replaced by Mg-rich phyllosilicates. Opaque nodules, which are common in chondrules in other chondrites, are absent. Most chondrules consist of irregularly shaped cores composed of forsterite and enstatite and phyllosilicate-rich outer zones (POZs) which surround the cores. In the cores and in the POZs, characteristic round objects are commonly observed. They consist largely of phyllosilicates, and their chemical compositions are significantly richer in Cr_2O_3 than any other phyllosilicates consisting of materials in the carbonate-poor lithology of Tagish Lake. The enrichment of Cr in these round objects is most consistent with their origin from Fe metal. That is, these round objects are pseudomorphs of opaque nodules, which were replaced by phyllosilicates during aqueous alteration. Most chondrules are fully or partly surrounded by fine-grained phyllosilicate-rich rims which exhibit much smoother surface compared with the matrix. The rims mainly consist of fine-grained phyllosilicates with minor amount of Fe-Mg carbonate, Fe-(Ni) sulfides, forsteritic olivine, and magnetite. Ca carbonate, which is commonly observed in matrix, is absent in the rims. In many cases, characteristic fractures run radially from the core/POZ interfaces and penetrate both POZs and rims, and always terminate at the rim/matrix interfaces.

Both of the two CAIs contain large amount of secondary minerals such as Ca carbonate, Mg-Ca carbonate, and phyllosilicates. One of them preserve the initial materials, Fe-poor spinel, as the second most abundant mineral, whereas the other only contains spinel as small relict grains. These two CAIs are also completely surrounded by fine-grained rims which are identical to those surround the chondrules in texture, mineralogy and chemical compositions. The radial fractures which start from the core/rim boundary and terminate at the rim/matrix boundary are also common in the

rims of CAIs.

Forsterite aggregates consist almost solely of small forsterite grains and have highly irregular shape compared with chondrules. They are compact aggregates of forsterite grains. The interspaces of forsterite grains are pores. In rare cases, small grains of magnetite or spinel fill these interspaces. All of the forsterite aggregates are surrounded by fine-grained rims which are identical to those surround the chondrules and CAIs in texture, mineralogy and chemical compositions. The radial fractures which start from the core/rim boundary and terminate at the rim/matrix boundary are also common in the rims of forsterite aggregates.

We found 55 matrix clasts which lack coarse components (chondrules, CAIs and forsterite aggregates). They consist of materials texturally and mineralogically identical to the fine-grained rims surrounding coarse components. They are commonly round in shape and basically smaller than those coarse components. We also found a large clast which contains three chondrules and three forsterite aggregates. The matrix of this large clast is identical to the matrix clasts described above. Chondrules in this clast have identical texture, mineralogy and chemical compositions to those of the chondrules in the host matrix; they consist of irregularly shaped cores and POZs. However, they have no fine-grained rims. Similarly, forsterite aggregates in the clast lack rims. The matrix of the clast exhibits fractures that run radially from the surfaces of the chondrules and forsterite aggregates and interconnect them. Most of the fractures terminate at the boundary between the clast and the host matrix.

Chapter 4: Discussions. The common occurance of the pseudomorphs of opaque nodules in both chondrule cores and POZs suggests that the POZs are altered zones which were formed by the replacement of opaque nodules, mesostasis and enstatite

preferentially from the peripheries of chondrules due to the introduction of fluids from outside. The altered zones and the rims are compositionally and texturally similar, although they exhibit some differences in secondary minerals. In comparison, the rims and the host matrix show more significant differences in bulk chemical composition, texture, and mineralogy. The observations suggest that the chondrules and the rims experienced aqueous alteration simultaneously, whereas the rims and the matrix experienced aqueous alteration under distinct conditions. I also found a clast that contains multiple coarse-grained components embedded in a matrix and numerous smaller matrix clasts. The coarse-grained components in the clast have no rims, and the matrices of the clasts are mineralogically identical to the rims.

The results suggest that the chondrules, other coarse-grained components, and their rims (generically referred to as chondrules/rims) and the clasts originated from a common precursor region in the meteorite parent body that was different from the location where the host meteorite was finally lithified. That is, the chondrules/rims are actually clasts produced by brecciation and later transported and incorporated into the present host matrix. The rims are, therefore, remnants of matrix material that formerly filled interspaces between the chondrules and other coarse-grained components. This model is essentially consistent with those previously proposed for the carbonate-rich lithology of Tagish Lake and the hydrated chondrules/rims in the Vigarano and Mokoia CV3 chondrites.

CONTENTS

1.

INTRODUCTION

1.1 Aqueous alteration in carbonaceous chondrites

Planetary materials, now we have in our solar system, are products formed through the evolution process of the solar system, thus they have information about the formation history of it. However, on the differenciated bodies such as plenets, elements in materials have been equilibrated and their original characteristics have been overprinted. In order to uncover the very first stage of the solar system, it is necessory to study the primitive materials that preserve their original information. Asteroids are much smaller than planets thus they are expected to contain primitive materials. However, it is not easy to reach them and obtain materials there; such missions are in proceed (ex. HAYABUSA mission). Then, the primitive materials we can handle include meteorites, interplanetary dust particles (IDPs), and micrometeorites (MMs). Their chemical compositions and orbits suggest that they are originated from asteroids. Among such materials, those include hydrous minerals are thought to be especially primitive considering that CI chondrites, the reprisentative of such hydrous planetary materials, have almost identical bulk chemical compositions to those of the sun. Hydrous meteorites, IDPs, and MMs are thought to have come from D type asteroids whose surface infrared spectrums show the presence of hydrous minerals and/or comets which are mixtures of rock and ice, however, we had not have any sample which are clearly from such parent bodies until recent years. In January in 2000, a meteorite fell on the frozen surface of Tagish Lake in Canada and was picked up immediately after the fall. The meteorite, named Tagish Lake, is thought to be the first sample from D type asteroids since it has similar surface infrared spectrum to that of the D type asteroid 308 Polyxo (Hiroi, 2003). Also, Tagish Lake has almost identical mineralogy to those of hydrous MMs, which consist approximately half of the MMs (Noguchi et al.,

2002). Consider with that hydrous asteroids can easily be crushed into tiny pieces by impacts thus significantly less amount of hydrous meteorites reach us (Tomeoka et al., 2003), there is a possibility that Tagish Lake is the representative material of hydrous asteroids. From these background, we intended to uncover the evolution process of the materials in the early solar system through a petrographical and mineralogical study of Tagish Lake carbonaceous chondrite.

1.2 Tagish Lake carbonaceous chondrite

Tagish Lake is an ungrouped type 2 carbonaceous chondrite that has experienced extensive aqueous alteration and has mineralogical and chemical similarities to CI and CM groups (e.g., Brown et al., 2000; Clayton and Mayeda, 2001; Keller and Flynn, 2001; Friedrich et al., 2002; Grady et al., 2002; Mittlefehldt, 2002; Noguchi et al., 2002; Zolensky et al., 2002; Nakamura et al., 2003; Bland et al., 2004; Izawa et al., 2010; Russell et al., 2010). Zolensky et al. (2002) described this meteorite as "a breccia at all scales" consisting of two major lithologies: carbonate-rich and carbonate-poor. More recent studies indicated that there are additional lithologies that exhibit differences in aqueous alteration mineralogy from these two major lithologies (e.g., Blinova and Herd, 2010; Izawa et al., 2010).

The mineralogy of Tagish Lake is most similar to those of CI chondrites. One of the major difference of Tagish Lake from CI chondrites is the presence of chondrules and other inclusions (e.g. CAIs); though their modal abundances are not as high as those in other types of carbonaceous chondrites. The oxygen isotopic composition of Tagish

Lake is not overlapped but most similar to those of CI chondrites (Clayton and Mayeda, 2001). Thus, Tagish Lake had been classified as "CI2" chondrite in the first several studies. Compared with CM chondrites, the mineralogy of Tagish Lake is significantly different. For example, the representative alteration product in CM chondrites, tochilinite, is absent. Also, the oxgen isotopic composition of Tagish Lake is far different from those of CM chondrites (Clayton and Mayeda, 2001). One of the resemblances to CM chondrites, and one of the remarkable characteristics, of Tagish Lake is that most chondrules and coarse-grained components are surrounded by thick, fine-grained rims (e.g., Zolensky et al., 2002).

1.3 Fine-grained rims in carbonaceous chondrites as a key to uncover the evolution process of the early solar system

Fine-grained rims surrounding chondrules and inclusions in unequilibrated chondrites have been studied by a number of researchers, but their origin is still controversial. The vast majority of researchers have supported the model that the rims were formed by the accretion of dust onto the surfaces of chondrules and inclusions in the solar nebula (e.g., Metzler et al., 1992; Cuzzi et al., 2005). However, there are also a few studies indicating that the rims resulted from parent-body processes (e.g., Sears et al., 1993; Tomeoka and Tanimura, 2000; Trigo-Rodriguez et al., 2006). Both of these types of model are briefly reviewed in Tomeoka and Ohnishi (2010). I consider that clarifying how the rims formed provides fundamental constraints on the processes that occurred in the solar nebula and in the early evolution of planetesimals.

The parent-body formation model proposed by Tomeoka and Tanimura (2000) for hydrated rims in the Vigarano CV3 chondrite is as follows. The chondrules, inclusions, and their rims are actually clasts that were produced by brecciation in a wet region of the meteorite parent body and subsequently transported and incorporated into the anhydrous matrix. Thus, the rims are remnants of matrix in the precursor region adhering to chondrules and inclusions. A more recent study of the Mokoia CV3 chondrite by Tomeoka and Ohnishi (2010) showed that the mineralogy and texture of most chondrules and inclusions, regardless of whether they are rimmed or not, are consistent with this formation model.

By studying the carbonate-rich lithology, Nakamura et al. (2003) found that the rims surrounding chondrules and the matrices of clasts consist of identical materials and suggested that the chondrules with their rims and the clasts were "part of earlier formed chondritic materials and from which they were excavated and incorporated into new locations" (page 97), which is consistent with the rim formation model proposed by Tomeoka and Tanimura (2000). In contrast, by observing the carbonate-poor lithology, Greshake et al. (2005) described that the rims are not genetically linked to the enclosed objects and show no evidence of fragmentation and concluded that "formation of the rims by accretion in the solar nebula most convincingly accounts for all textural, mineralogical, and compositional characteristics of the fine-grained rims" (page 1429).

I was motivated by the fact that these contrasting views were proposed for the two major lithologies of the same meteorite. The two lithologies have some differences in their texture and mineralogy (e.g. Zolensky et al., 2002), but these differences are minor comparing with those with other chondrties. They both consist of one single meteorite

and their interface is gradational (Zolensky et al., 2002). From these observation, one would naturally expects that these two lithologies have certain links with each other in their formation histories; however, significantly distinct formation models of fine-grained rims for each of them have been proposed as described above. Nakamura et al. (2003) pointed out that the earlier-formed body (from which clasts were originated) could be the Tagish Lake parent body itself since the mineralogy of the clast (in the carbonate-rich lithology) is similar to that of matrix material in the carbonate-poor lithology. However, no study on the carbonate-poor lithology which considers that possibility has been done.

In this paper, I present the results of detailed petrographic and mineralogical investigation of the carbonate-poor lithology of the Tagish Lake meteorite. My goal in this study is to find any evidence indicating the processes and conditions of rim formation, to determine which of the above or other models of rim formation most consistently explains the mineralogical and petrographic characteristics of the rims and other components, and to elucidate the formation history of the Tagish Lake carbonate-poor lithology.

2.

MATERIALS AND METHODS

The samples used for this study are two polished thin sections (total area of 114 mm^2) from the Tagish Lake carbonaceous chondrite. They were studied using an optical microscope, a JEOL JSM-6480LAII scanning electron microscope (SEM) equipped with an energy dispersive X-ray spectrometer (EDS), and a JEOL JXA-8900 electron probe microanalyzer (EPMA) equipped with wavelength-dispersive X-ray spectrometers (WDS). For most SEM observations, I used back-scattered electron imaging. EDS analyses were obtained at 15 kV and 0.6 nA, and WDS analyses at 15 kV and 6 nA. Data corrections were made by the ZAF method for the EDS analysis and by the Bence-Albee method for the WDS analysis except for metals, whose data corrections were made by the ZAF method. Standards used for the analyses (and elements analyzed) were: jadeite (Na), periclase (Mg), corundum (Al), quartz (Si), $KTiPO_5$ (P), pyrite (S), $KTiPO_5$ (K), wollastonite (Ca), rutile (Ti), eskolaite (Cr), manganosite (Mn), hematite (Fe), and NiO (Ni). For the analysis of each mineral, I use a focused electron beam of ~2 μm in diameter. For the bulk analysis of fine-grained rims, clasts, and matrix, I used a defocused electron beam of 5−10 μm in diameter; areas including grains larger than 5 μm were avoided. For the analysis of phyllosilicates, I mostly used the SEM-EDS, because the phyllosilicates are very fine-grained, porous and commonly intimately associated with other mineral grains; therefore, I needed to locate them directly by BSE imaging. The X-ray elemental maps were acquired on the SEM at 15 kV and 0.6 nA using an electron beam of ~2 μm in diameter.

For the measurements of the modal abundances of chondrules, Ca-Al-rich inclusions, forsterite aggregates, and clasts in the meteorite, the BSE images were used. These objects were colored on the BSE images, and the colored areas were calculated as a percentage of the whole area of the sections using the Adobe Photoshop software

package. For measurements of minor mineral grains in the altered zones and rims of chondrules and the matrices of clasts and host meteorite, the same basic procedure was followed. The BSE images of randomly selected areas, each of which was approximately $40 \times 30\ \mu m^2$, were obtained from those objects. Then, minor mineral grains in these images were colored, and the colored areas were calculated as a percentage of the whole image. The modal abundances of pseudomorphs of opaque nodules in chondrules were calculated by a same method.

3.

RESULTS

3.1 General petrography

The thin sections of Tagish Lake consist of a dominant matrix (84.1 vol.%) and 87 embedded chondrules (50–660 μm in diameter with an average of 190 μm; 11.1 vol.%), 2 Ca-Al-rich inclusions (CAIs) (500 and 370 μm in diameter; 0.4 vol.%), and 14 forsterite aggregates (50–660 μm in diameter with an average of 180 μm; 2.1 vol.%). The forsterite aggregates are irregularly shaped compact aggregates consisting of small grains (1–40 μm) of almost pure forsterite ($Fo_{>99.5}$), with very minor amounts of small grains (<1–5 μm in diameter) of magnetite and spinel. They were first described by Simon and Grossman (2003), but most other researchers appear to have included them in chondrules. Here I distinguish them from chondrules, since they are clearly distinct in mineralogy and texture.

In addition, I found one lithic fragment (~450 μm in diameter; 0.4 vol.%) that contains multiple chondrules and forsterite aggregates embedded in a matrix and 55 lithic fragments (100–250 μm in diameter; 1.9 vol.%) that consist entirely of a fine-grained matrix material. The matrices of all these fragments are distinctly brighter in back-scattered electron images, less porous, and smoother on the surfaces than the host matrix (Fig. 1a–c). I consider all of these fragments to be clasts that were produced by brecciation. While relatively large clasts (>100 μm in diameter) generally exhibit round shapes (Fig. 1a), there are also abundant irregularly shaped clasts. In addition, numerous smaller clasts (<100 μm in diameter) consisting entirely of the same fine-grained matrix material are scattered throughout the host matrix.

Table 1. Modal abundances of minerals in POZs (altered zones), rims, matrices of clasts, and host matrix (area%).

	No. of chondules/clasts	No. of areas*	Forsterite	Magnetite	Fe-(Ni) sulfides	Ca carbonate	Fe-Mg carbonate	Total
POZs (altered zones)	5	7	0.1	2.0	0.4	0.0	0.3	2.8
Rims	5	7	0.3	0.2	2.5	0.0	4.3	7.3
Matrices of clasts	6	6	0.7	0.7	1.2	0.0	4.2	6.8
Host matrix		14	1.7	2.2	0.5	1.1	2.9	8.4

*Each area is approximately 1200 μm^2

Fig. 1

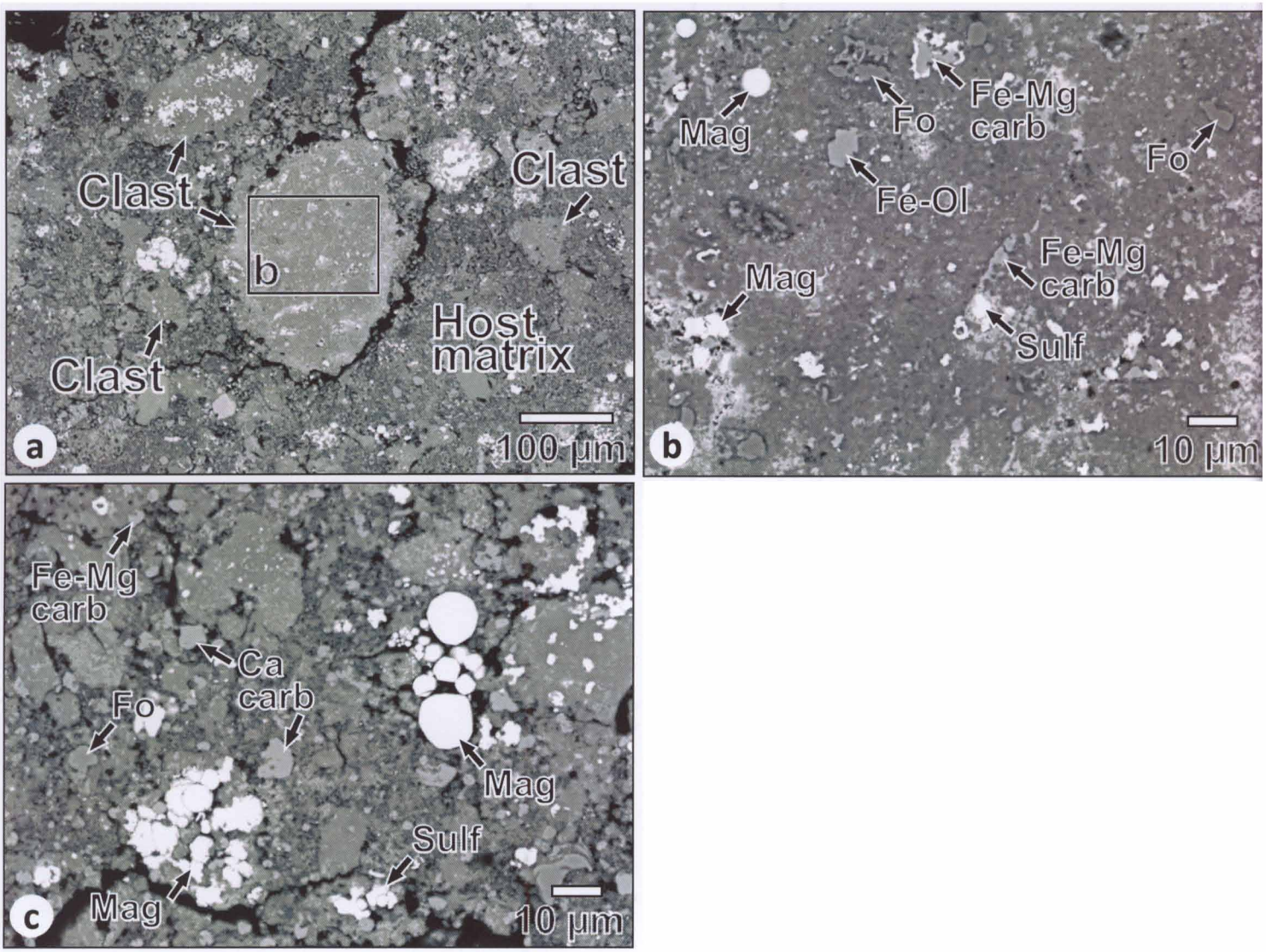

Fig. 1 (a) Back-scattered electron image of matrix clasts embedded in the matrix of the Tagish Lake meteorite. The clasts exhibit a distinctly brighter appearance than the host matrix. (b) Image of boxed area b in (a) showing that the clast consists of fine grains of phyllosilicates (dark background) and minor Fe-Mg carbonate (Fe-Mg carb), Fe-(Ni) sulfides (Sulf), forsterite (Fo), magnetite (Mag), and Fe-rich olivine (Fe-Ol). (c) Image of a portion of the host matrix consisting of fine grains of phyllosilicates (dark background) and minor Fe-Mg carbonate, magnetite, forsterite, Ca carbonate (Ca carb), and Fe-(Ni) sulfides. The matrix has abundant pores and an uneven surface, compared to the clast shown in (b). The magnetite forms framboidal aggregates.

3.2 Matrix

The matrix is characterized by abundant pores (1–5 μm in diameter) and an uneven surface (Fig. 1c). The matrix mainly consists of fine-grained phyllosilicates, with minor amounts of small grains (<1–20 μm in diameter) of Fe-Mg carbonate, magnetite, forsteritic olivine, Ca carbonate, and Fe-(Ni) sulfides (in order of abundance) (Fig. 1c); modal abundances of these minerals are shown in Table 1. Zolensky et al. (2002) identified that the Fe-Mg carbonate is siderite and Fe-(Ni) sulfides are pyrrhotite and pentlandite. Izawa et al. (2010) identified that the Ca carbonate is calcite. Magnetite commonly occurs as spherical particles (<1–20 μm in diameter) and framboidal aggregates. The results of defocused beam analyses of the matrix (Table 2) show good agreement with those reported by Greshake et al. (2005). The low analytical total can probably be ascribed to the highly porous nature in addition to the presence of hydrous phyllosilicates. The texture, mineralogy, and chemical composition of the matrix of my sample are basically consistent with those reported from the carbonate-poor lithology of Tagish Lake (Zolensky et al., 2002; Greshake et al., 2005; Bland et al., 2004). Thus, I identify my sample as belonging to the carbonate-poor lithology. Previous TEM (Keller and Flynn, 2001; Zolensky et al., 2002; Greshake et al., 2005) and X-ray diffraction (Bland et al., 2004; Izawa et al., 2010) studies reported that the phyllosilicates in the matrix of the carbonate-poor lithology are Mg-rich smectite (saponite) and serpentine.

3.3 Chondrules

3.3.1 Cores

60 (69%) of the 87 chondrules studied are of porphyritic olivine-pyroxene (POP) type and consist mainly of forsterite and enstatite phenocrysts (5–200 μm in diameter). 20 (23%) are of porphyritic olivine type and consist mainly of forsterite phenocrysts. The rest (8%) are of porphyritic pyroxene and barred olivine types. In the POP type chondrules, there is a tendency for forsterite to be concentrated in the cores, whereas enstatite is abundant in the outer zones. Figures 2–4 show back-scattered electron images of POP type chondrules. Most of the forsterite phenocrysts are nearly pure forsterite ($Fo_{>99}$), which is one of the characteristic features of this meteorite, and show almost no evidence of alteration. On the other hand, most of the enstatite phenocrysts have been replaced to various extents by phyllosilicates, which typically occur as narrow fibrous grains with abundant pores (Fig. 2c and e; Table 3). The mesostases were completely replaced by the same phyllosilicates. Diopside phenocrysts, which are common in chondrules of most other carbonaceous chondrites, are absent. Diopside only occurs sparsely as small grains (<10 μm in diameter) in the phyllosilicates replacing enstatite and/or mesostasis. Magnetite mainly occurs as framboidal aggregates and stacks of platelets (placquettes) in the interstices of phenocrysts. Opaque nodules, which are normally common in chondrules in other chondrites, are absent except for very small metal inclusions (≤5 μm in diameter) inside forsterite phenocrysts.

In the (Si+Al)–Fe–Mg ternary diagram (Fig. 5a), most of the analyses of the phyllosilicates plot around a Mg-rich range of the pyroxene solid solution line whose (Si+Al)/(Fe+Mg) ratio is 1. These phyllosilicates probably correspond to the Mg-rich

Fig. 2

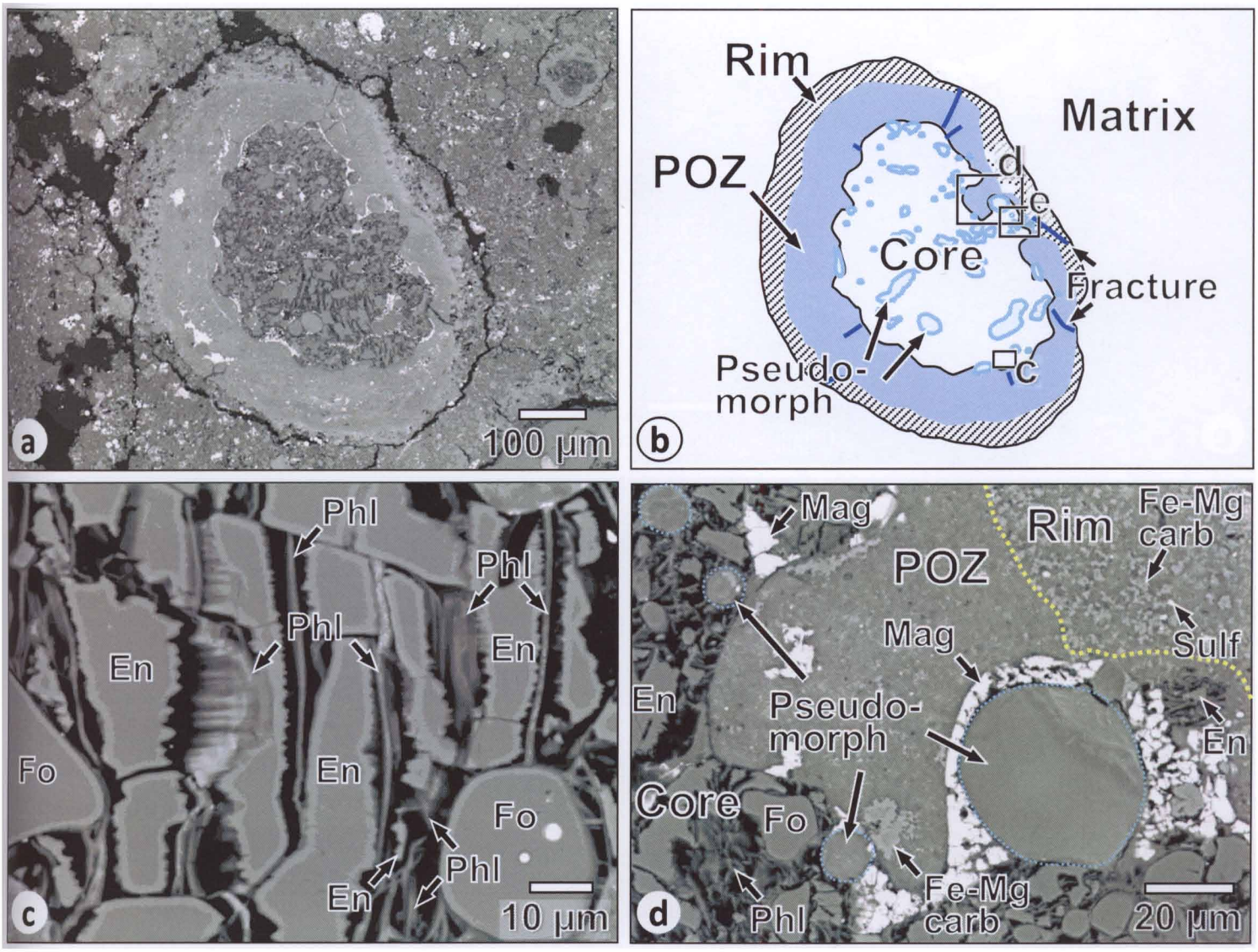

Fig. 2 (a) Back-scattered electron image of a chondrule with a fine-grained rim. (b) Illustration of (a) showing the chondrule core, phyllosilicate-rich outer zone (POZ), and rim. Pseudomorphs of opaque nodules are outlined by light blue lines. Fractures are indicated by dark blue lines. (c) Image of boxed area c in (b) showing that enstatite (En) grains were partially replaced by phyllosilicates (Phl) and exhibit jagged outlines, whereas forsterite (Fo) grains show no evidence of such replacement. (d) Image of boxed area d in (b) showing the core, POZ, and rim. Pseudomorphs of opaque nodules are outlined by light blue dotted lines. The large pseudomorph on the right is partly rimmed by magnetite (Mag). Fine grains of Fe-Mg carbonate (Fe-Mg carb) are abundant in the rim.

Fig. 2 continued

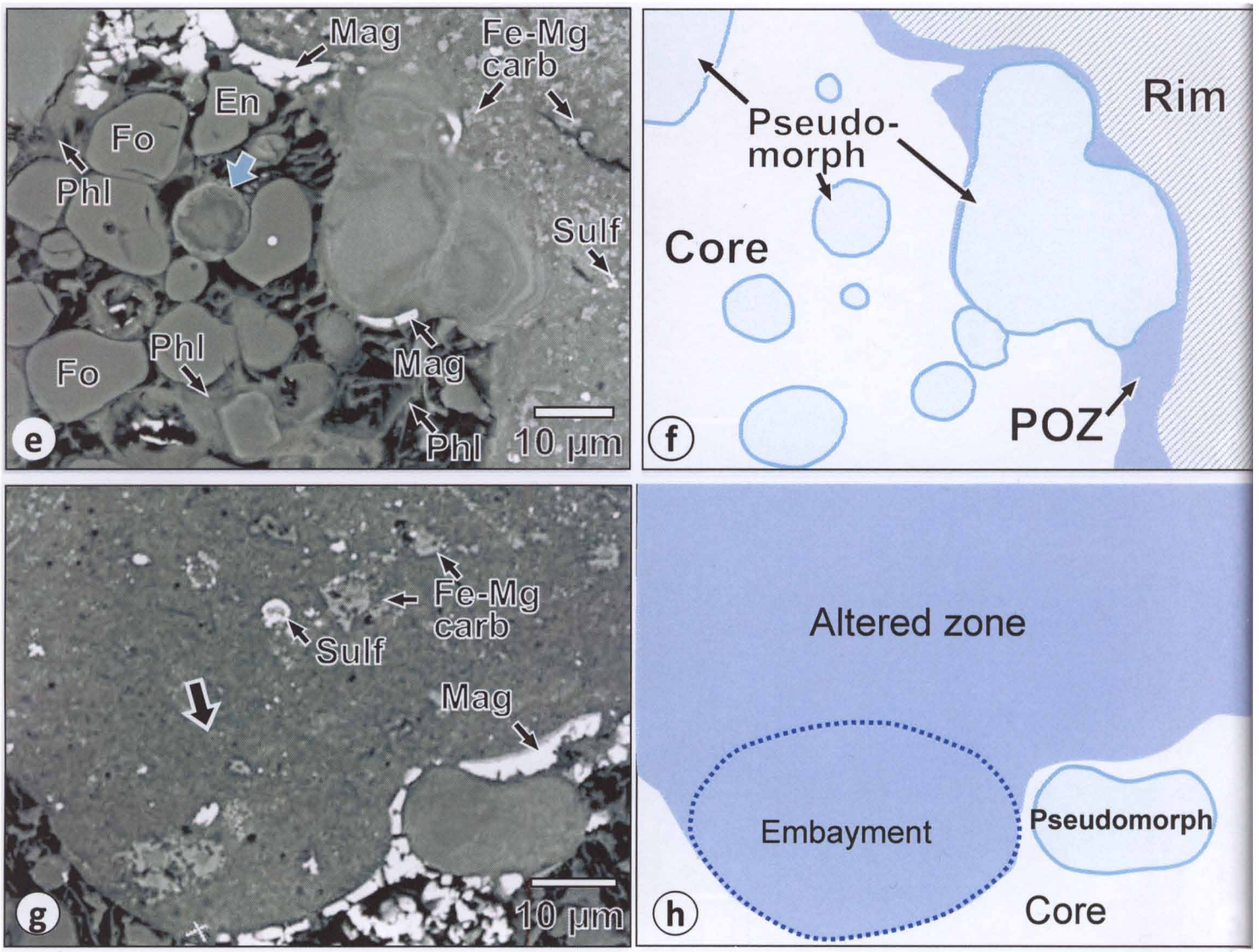

Fig. 2 continued. (e), (f) Image of boxed area e in (b) and its illustration, showing pseudomorphs of opaque nodules in the chondrule core and POZ. A pseudomorph outlined by Fe-rich phyllosilicates (bright) is indicated by a light blue arrow. (g), (h) Image and its illustration of the periphery of the core showing the embayment and pseudomorph occurring next to each other. Sulf=Fe-(Ni) sulfides.

Fig. 2 continued

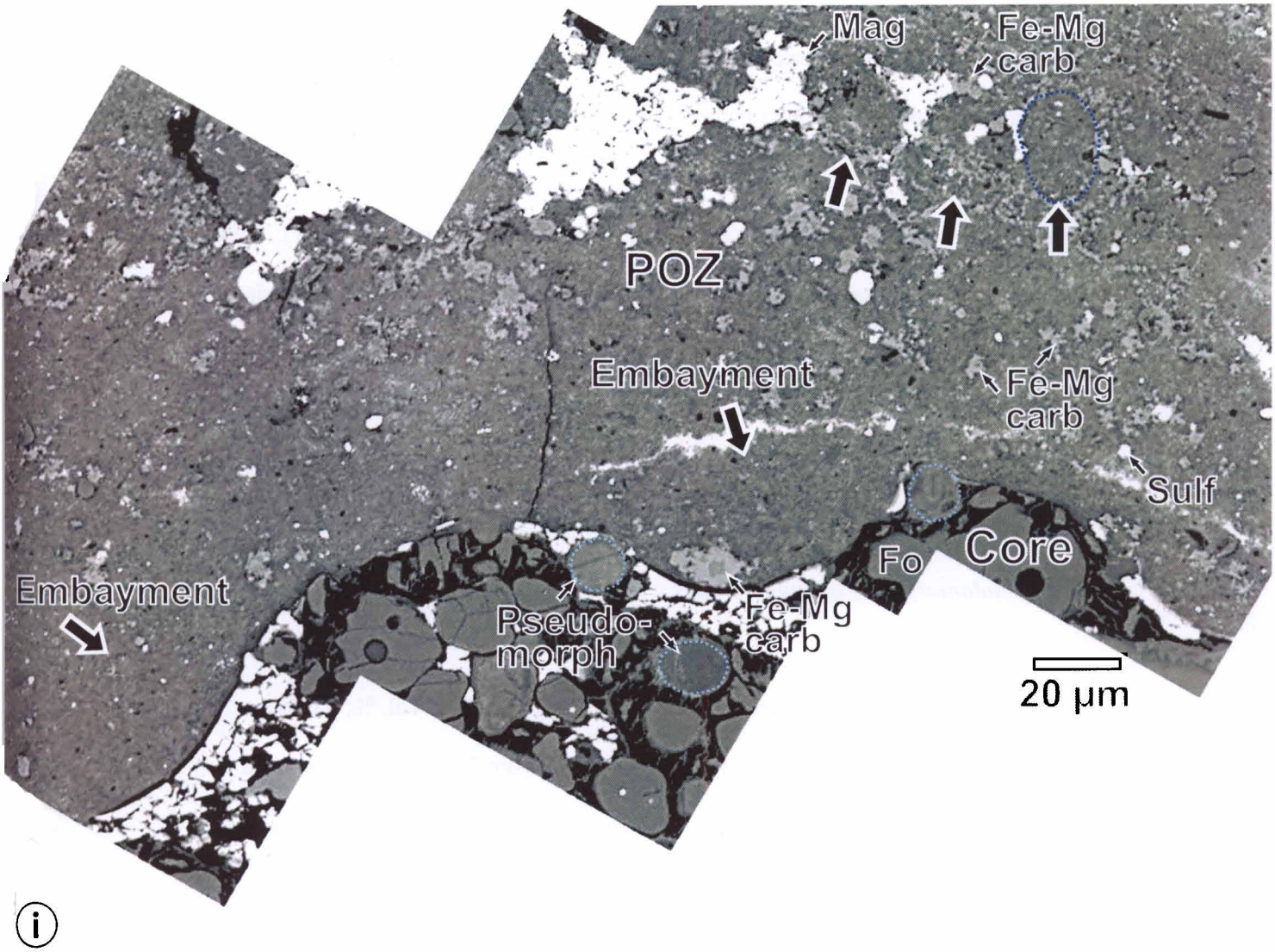

Fig. 2 continued. (g) Image of the periphery of the core of(a). Characteristic embayments are indicated by thick arrows. Round objects outlined by magnetite and Mg-Fe carbonate in the POZ are also indicated by thick arrows. On e of them is outlined by blue dotted line.

saponite and serpentine reported by Zolensky et al. (2002) as the typical phyllosilicates in the carbonate-poor lithology (analysis 1 in Table 3 in their paper) and to the Mg-rich phyllosilicates reported by Greshake et al. (2005) as the alteration products replacing chondrule silicates and mesostases (Figs. 2b, 3, Tables 2, and 3 in their paper). These phyllosilicates in my sample are also referred to as Mg-rich phyllosilicates. Their porous nature is probably the main reason for the unusually low analytical totals (69.3 wt.% on average).

3.3.2 Pseudomorphs of opaque nodules

70 (81%) of the 87 chondrules contain 1 to 79 (0.3 to 22.4 vol. %; 5.0 % on average) round pseudomorphs that range in diameter from 3 to 70 μm and consist mainly of phyllosilicates (Figs. 2d–f, 3a–f). These pseudomorphs may correspond to what Greshake et al. (2005) described as follows: "several Fe, Ni metal inclusions in the forsteritic olivine are replaced by alteration products" (page 1417; their compositions are in Table 4 in their paper), although no images for the inclusions are available. Otherwise, there are no previous reports of such pseudomorphs in Tagish Lake chondrules; however, here I emphasize that they are very abundant constituents of the chondrules. Pseudomorphs in each chondrule consist 12 vol. % in average. The pseudomorphs have smooth surfaces and are often outlined by narrow rims of Fe-rich phyllosilicates (typically ~1 μm in thickness) (Fig. 2e) and occasionally magnetite (typically 1–3 μm in thickness) (Fig. 3e). The pseudomorphs commonly contain magnetite grains (<1–10 μm in diameter) (Fig. 3b, e and f) and very small Fe sulfide

grains (<1 μm in diameter). In some cases, the pseudomorphs consist largely of framboidal magnetite, with minor amounts of phyllosilicates (Fig. 3g-i). From these observations, I conclude that these pseudomorphs were formed by replacing opaque nodules, which had formerly consisted largely of Fe-(Ni) metal and/or Fe-(Ni) sulfides.

The pseudomorphs are similar in chemical composition to those of the Mg-rich phyllosilicates replacing enstatite and mesostases, although the former are slightly more Fe-rich and show wider variations in Fe content (Fig. 5b; Table 3). A notable characteristic of the pseudomorphs is the distinct enrichment of Cr_2O_3 (up to 4.87 wt.% with an average of 1.59 wt.%; Table 3) compared to any other phyllosilicates in Tagish Lake. The chromium was probably inherited from metal in the opaque nodules. Using EPMA, I analyzed one of the small kamacite inclusions (~5 μm in diameter; the largest one found) contained inside a forsterite phenocryst and found that it contains 0.84 wt.% Cr (Fe: 92.7, Ni: 6.33, and P: 0.14 in wt.%); the Cr content is comparable to those of metals in CO (e.g., Kimura et al., 2008) and CV (e.g., Fuchs and Olsen, 1973) chondrules. Tomeoka and Ohnishi (2011) reported that similar pseudomorphs after opaque nodules, which consist largely of a phyllosilicate (saponite), are common in chondrules in an aqueously altered clast in the Mokoia CV3 chondrite and that they are also characterized by high Cr_2O_3 contents (~3 wt.%) (Figs. 2f, 3d, 4c, and analyses 3 and 4 in Table 1 in their paper). As the case of Ni content in more extensively altered metals which is significantly higher than those in less altered metals, Cr contents in (precursive) metal became relatively higher during aqueous alteration due to the lost of Fe.

Fig. 3

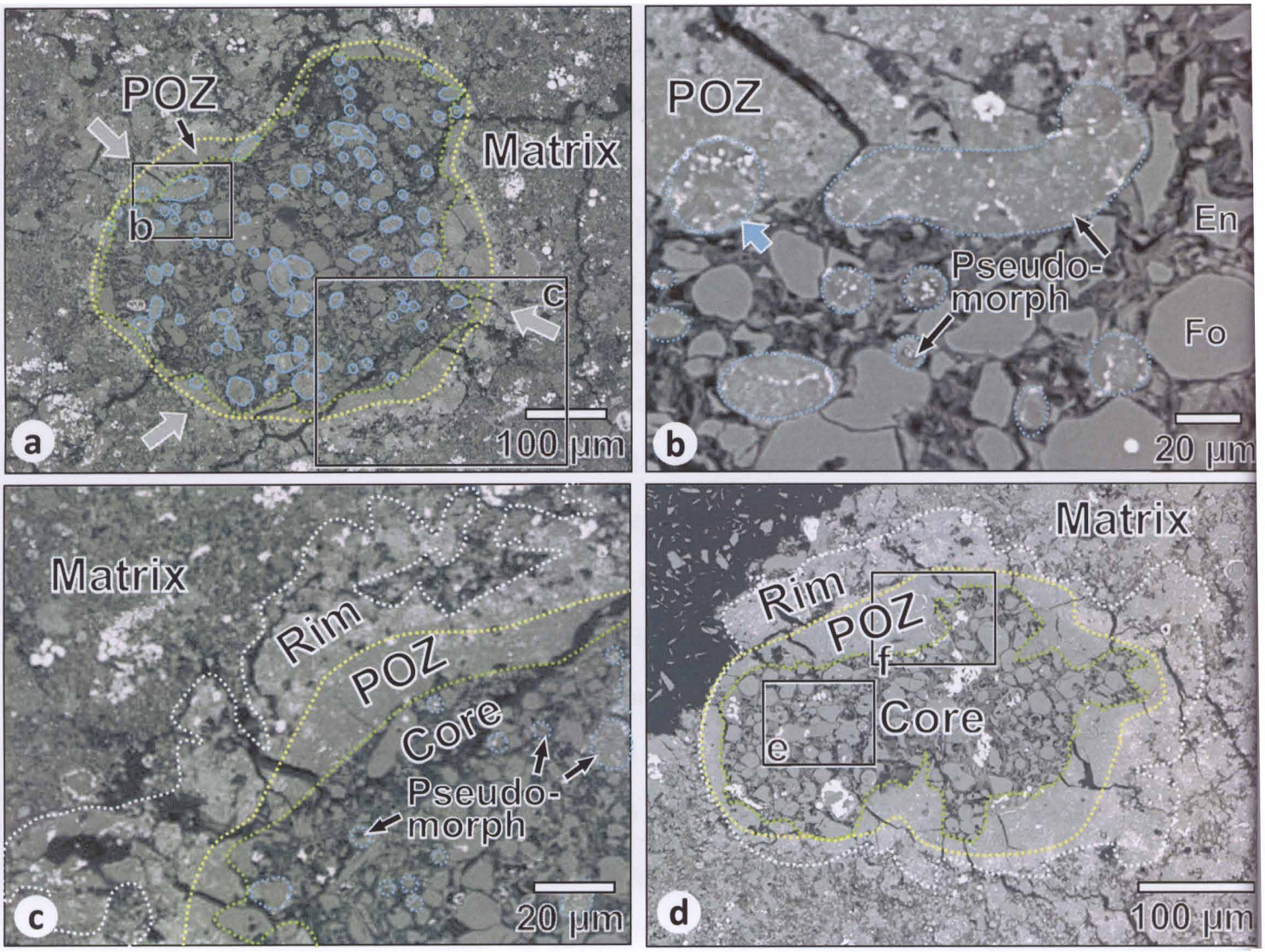

Fig. 3 (a) Back-scattered electron image of a chondrule that contains 79 and 7 pseudomorphs of opaque nodules (outlined by light blue lines) in its core and POZ, respectively. The chondrule core and POZ are outlined by green and yellow dotted lines, respectively. The rim is largely very thin and exhibits a very irregular outline; thus, it was not outlined. Some of the radial fractures that run through the POZ and rim are indicated by gray arrows. (b) Image of boxed area b in (a) showing pseudomorphs of opaque nodules (outlined by light blue dotted lines) in the core and POZ. The pseudomorphs contain fine grains of magnetite and Fe-(Ni) sulfides (bright specks). Note that a pseudomorph (indicated by a light blue arrow) occurs within the POZ. (c) Upside down image of boxed area c in (a) showing the core, POZ, rim, and matrix. The rim/matrix boundary (white dotted line) is very irregular. (d) Back-scattered electron image of a chondrule with a rim. The core is highly irregular in shape whereas the POZ is relatively smooth.

Fig. 3 continued

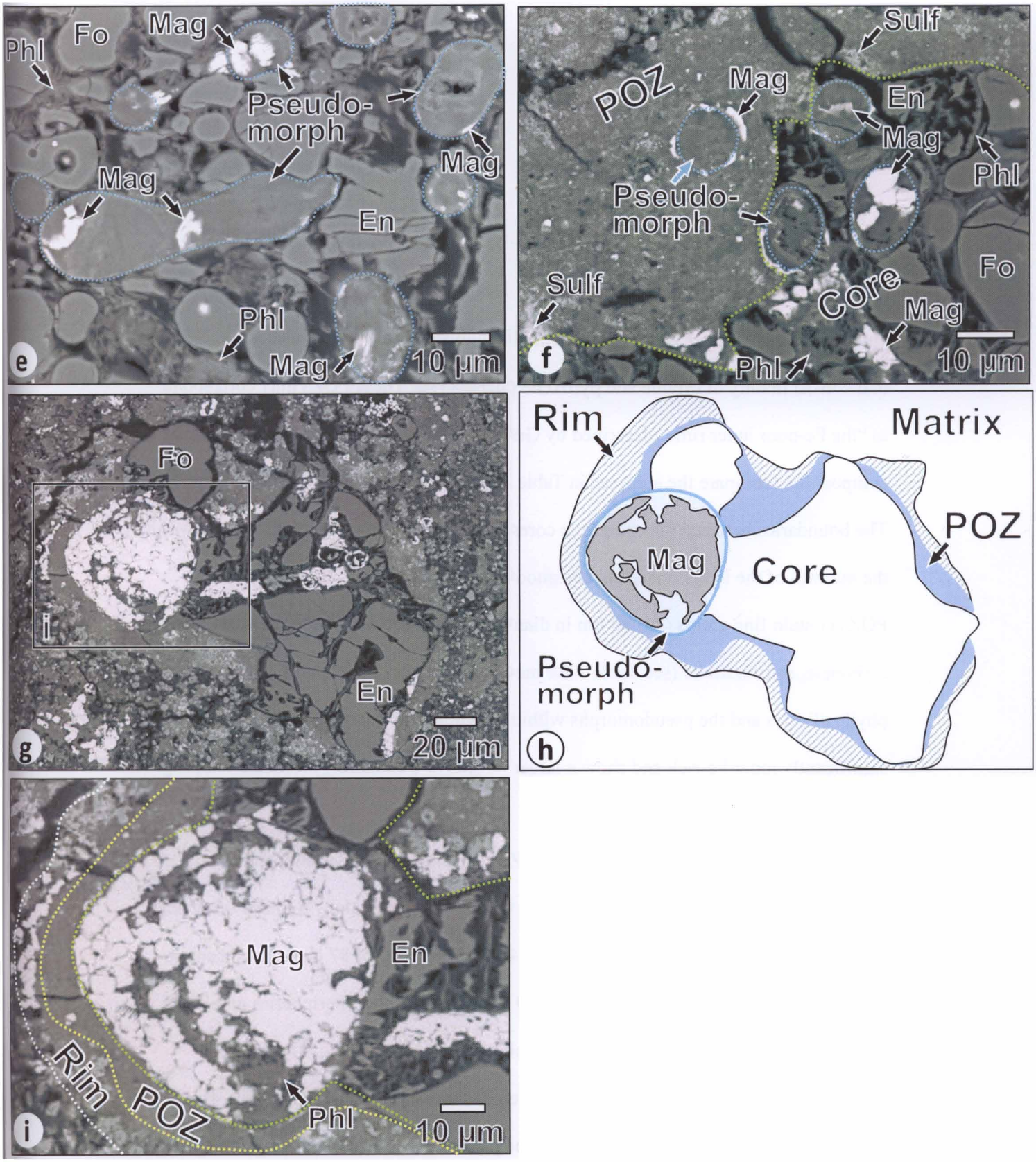

Fig. 3 continued. (e) Image of boxed area e in (d) showing that pseudomorphs contain magnetite (Mag) grains. (f) Image of boxed area f in (d). Note that a pseudomorph outlined by magnetite (indicated by a light blue arrow) is isolated in the POZ. The pseudomorphs in the core contain magnetite grains. Fo=forsterite, En=enstatite, Di=diopside, Sulf=Fe-(Ni) sulfides.

(g) Back-scattered electron image of a chondrule with a rim. . The chondrule core and POZ are outlined by green and yellow dotted lines, respectively. (h) Schematic view of (g). (i) Enlarged image of a pseudomorph of an opaque nodule that consists largely of framboidal magnetite and minor phyllosilicates (Phl). Fo=forsterite, En=enstatite, Mag=magnetite.

3.3.3 Phyllosilicate-rich outer zones

81 (93%) of the 87 chondrules have 5–100 μm thick phyllosilicate-rich zones along their margins (Figs. 2a, b, 3a, and 4a). I tentatively refer to these zones as phyllosilicate-rich outer zones (POZs) and distinguish them from the chondrule cores that consist mainly of olivine and pyroxene phenocrysts. These POZs may correspond to "the Fe-poor inner rims" described by Greshake et al. (2005), since they are similar in composition (compare the analyses in Table 2 to the analyses in Table 5 in their paper). The boundaries between the chondrule cores and the POZs are generally irregular, while the outlines of the POZs are relatively smooth (see Fig. 2a and b, for example). The POZs contain fine grains (<1–10 μm in diameter) of magnetite, Fe-(Ni) sulfides, Fe-Mg carbonate, and forsterite (see Table 1 for modal abundances). Compared to the Mg-rich phyllosilicates and the pseudomorphs within the chondrule cores, the POZs are significantly more Fe-rich and show a larger range of Fe contents (Tables 2 and 3; Fig. 5a–c).

My observations revealed that the POZs also contain round pseudomorphs of opaque nodules, which are identical in size, texture, and mineralogy to those occurring within the chondrule cores (Figs. 3b, f, and 4b–f). 75 (86 %) of 87 chondrules contain 1 to 26 pseudomorphs (0.5 to 24.0 vol. %; 7.9 in average) in their peripheries and POZs. While the pseudomorphs occur as isolated objects in the POZs (Fig. 3f), they also commonly occur near the boundaries between chondrule cores and POZs (Fig. 4b, c, and e). In back-scattered electron images, the pseudomorphs can be distinguished from the surrounding POZ material by their smooth surfaces and narrow rims of Fe-rich phyllosilicates and/or magnetite (Figs. 2d, e, and 3f). However, in some cases, they are

Fig. 4

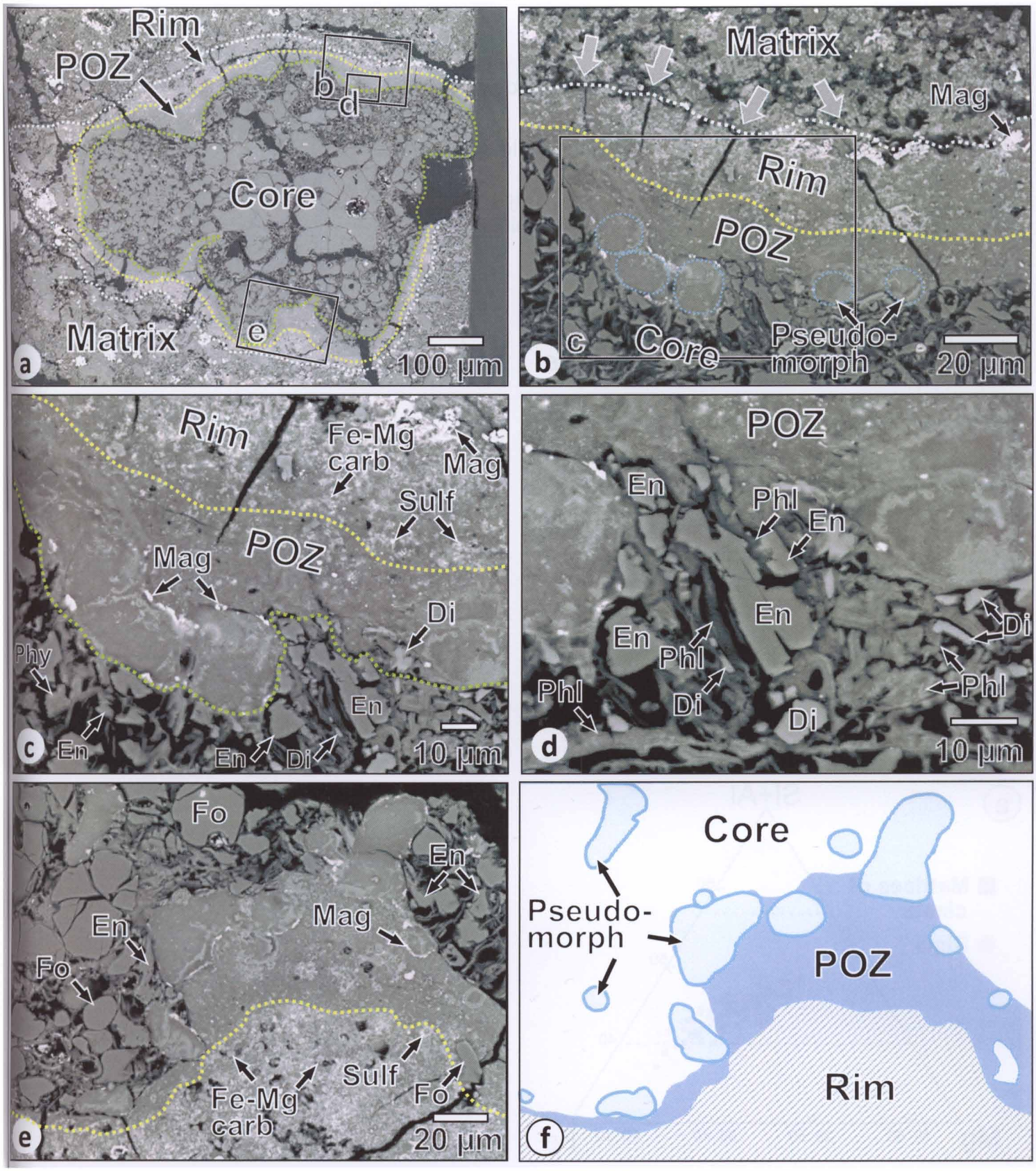

Fig. 4 (a) Back-scattered electron image of a chondrule with a rim. (b) Image of boxed area b in (a) showing the core, POZ, rim, and matrix. Pseudomorphs of opaque nodules are outlined by light blue dotted lines. Fractures are indicated by gray arrows. (c) Image of boxed area c in (b). The rim exhibits brighter appearance compared to the POZ due to the presence of Fe-Mg carbonate and Fe- (Ni) sulfides. (d) Image of boxed area d in (a) showing the periphery of the core. Enstatite is largely replaced by phyllosilicates. Di occurs as fine grains in the phyllosilicates. (e), (f) Image of boxed area c in (a) and its illustration, showing that pseudomorphs (outlined by light blue lines) occur in the core and POZ. Fe-Mg carbonate (Fe-Mg carb) and Fe-(Ni) sulfides (Sulf) are abundant in the rim. Fo=forsterite, En=enstatite, Mag=magnetite, Fe-Mg carb=Fe-Mg carbonate, Sulf=Fe-(Ni) sulfides, Di=diopside, Phl=phyllosilicates.

Fig. 5

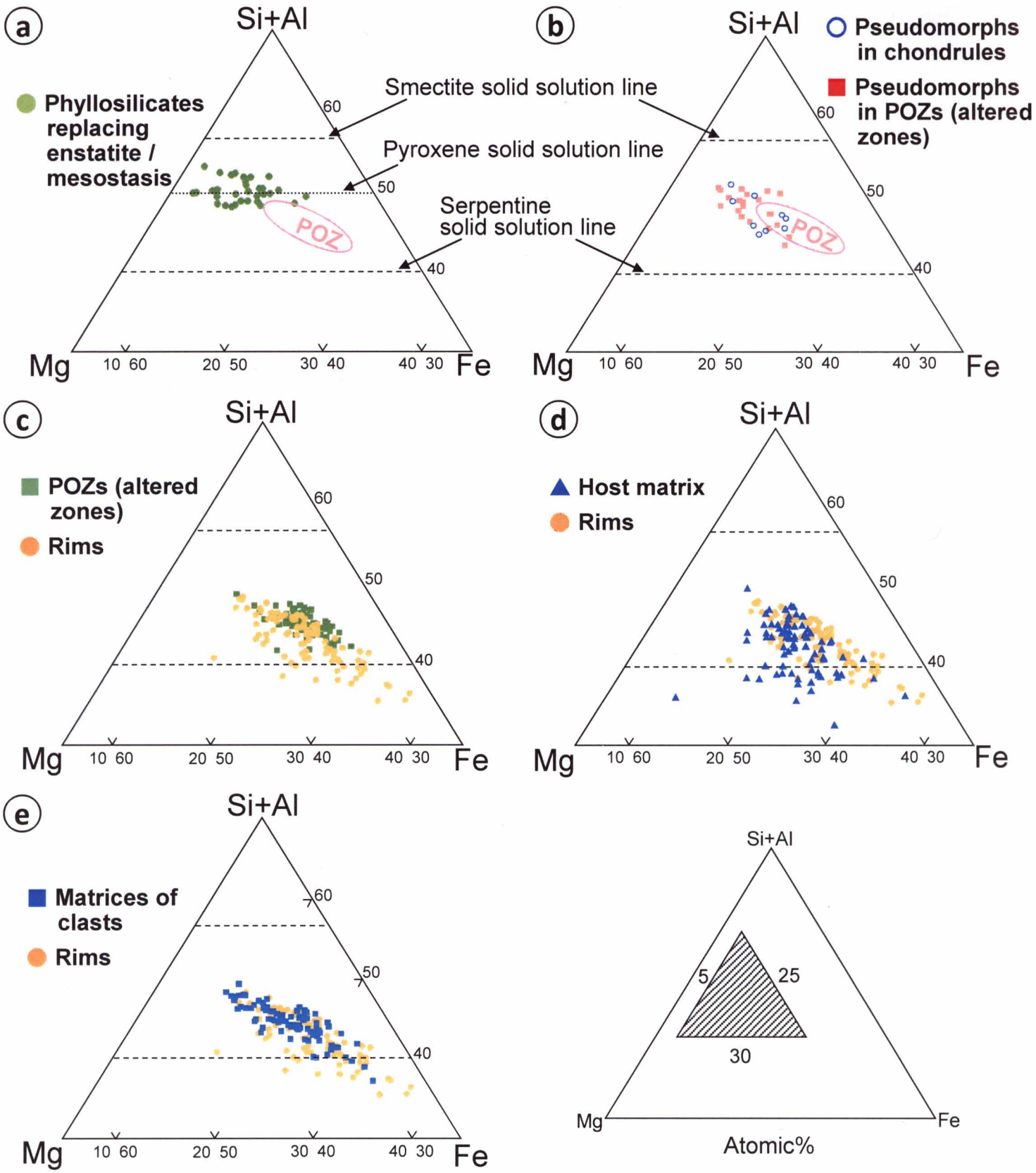

Fig. 5 (a) Defocused beam analyses of phyllosilicates replacing enstatite and mesostases in chondrules. Plotted are 28 analyses from 2 chondrules. Indicated by the pink ellipse is the main area of analyses of POZs. (b) Defocused beam analyses of pseudomorphs in chondrule cores and POZs. Plotted are 21 analyses from 10 chondrules for the pseudomorphs in the cores and 9 analyses from 5 chondrules for the pseudomorphs in the POZs. (c) Defocused beam analyses of POZs and rims. (d) Defocused beam analyses of rims and host matrix. (e) Defocused beam analyses of rims and matrices of clasts. The numbers of analyses and analyzed objects used for plotting are: 75 and 16 for POZs, 78 and 17 for rims, 84 and 17 for matrices of clasts, and 84 (analyses) for host matrix.

Fig. 6

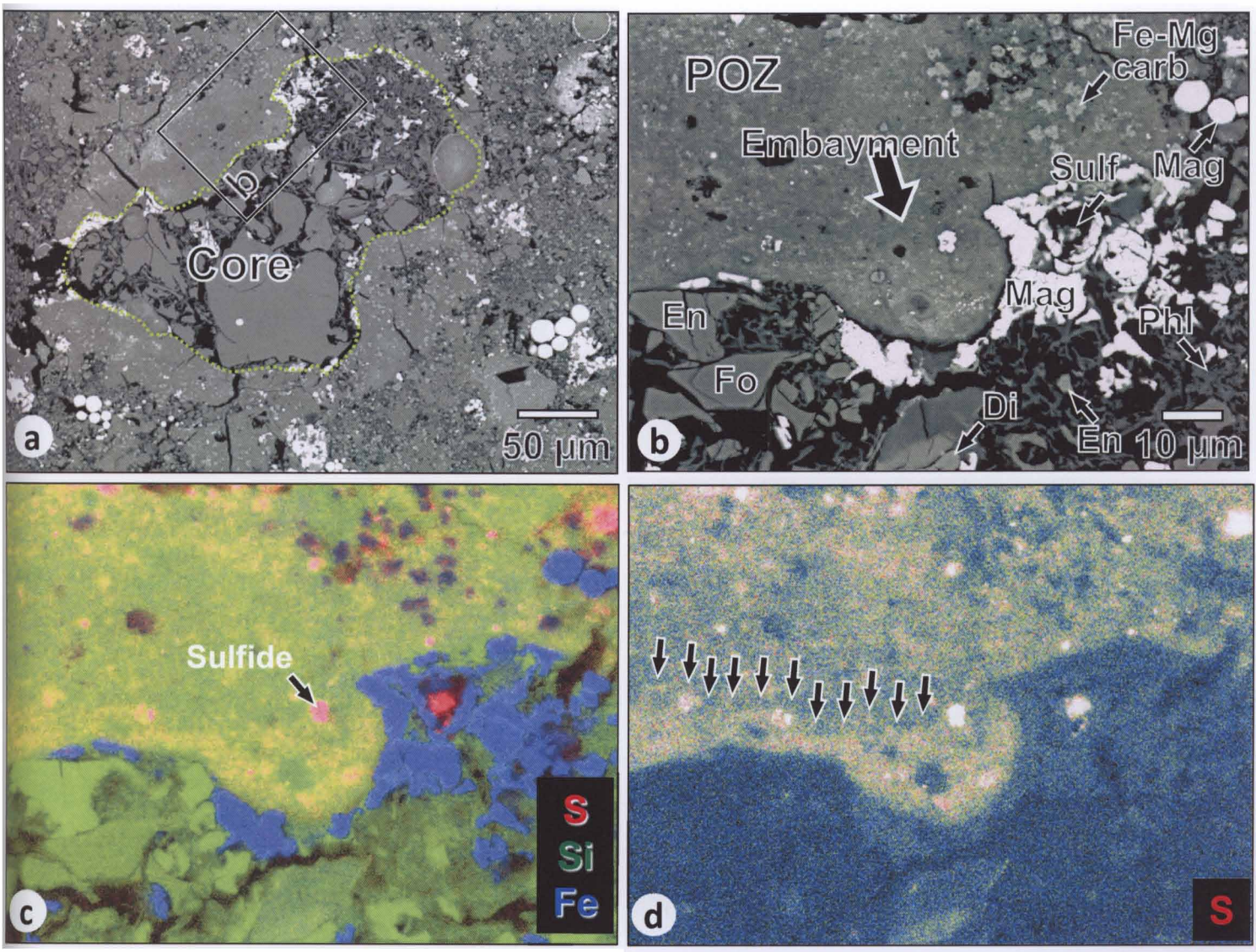

Fig. 6 (a) Back-scattered electron image of a chondrule . (b) Image of boxed area b in (a) showing the chondrule core/POZ boundary which exhibit a characteristic round depression (embayment) outlined by magnetite (Mag). (c) Combined X-ray elemental map of the area in (b). Pink spots correspond to sulfide. Red=S, Green=Si, Blur=Fe. (d) X-ray elemental map of sulfur of the area in (b) showing that sulfur is highly concentrated along the inner surface of the embayment. Fo=forsterite, En=enstatite, Di=diopside, Sulf =Fe-(Ni) sulfides, Fe-Mg carb=Fe-Mg carbonate, Phl=phyllosilicates.

Fig. 7

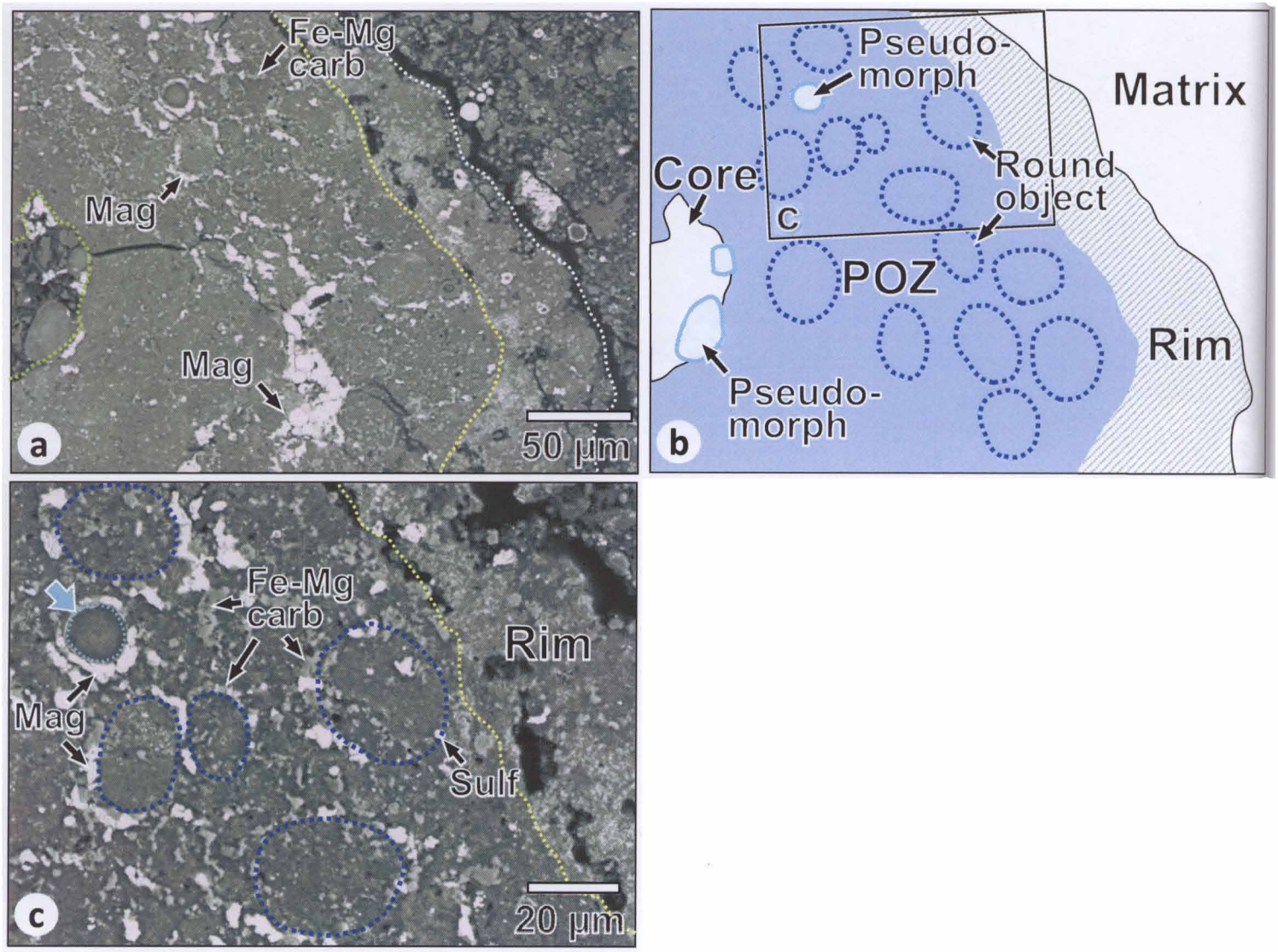

Fig. 7 (a) Back-scattered electron image of a portion of a chondrule having a thick POZ. In the POZ, characteristic round objects outlined by magnetite (Mag) and Fe-Mg carbonate (Fe-Mg carb) (both appear bright in the image) are abundant. (b) Illustration of (a) showing the chondrule core, POZ, rim, and matrix. The round objects are outlined by dark blue dotted lines. Pseudomorphs of opaque nodules are outlined by light blue lines. (c) Image of boxed area c in (b) showing that the round objects, some of which are outlined by dark blue dotted lines, are rimmed by magnetite and Fe-Mg carbonate. Also note that a pseudomorph outlined by magnetite (indicated by a light blue arrow) occurs together with the round objects in the POZ.

partially degraded and can barely be distinguished. Chemical compositions of the pseudomorphs in the POZs are identical to those of the pseudomorphs in the chondrule cores (Table 2; Fig. 5b).

Aside from these pseudomorphs, I found characteristic curved depressions (embayments) commonly occurring along the surfaces of the chondrule cores (Fig. 6a and b). These embayments are similar in size and shape to the pseudomorphs and are partly rimmed by magnetite, mostly along the boundaries between chondrule cores and POZs (Fig. 6a). The material inside these embayments is almost identical in chemical composition to the surrounding POZ material, although the X-ray elemental mapping showed that some of them are enriched in S (Figs. 2g-i, 6c, and d). Beside these embayments, there are also characteristic round objects (15–50 μm in diameter) that are outlined by fine-grained magnetite and/or Fe-Mg carbonate in areas apart from the chondrule core/POZ boundaries (Figs. 2h, 7a–c). These round objects are also similar in size and shape to the pseudomorphs, but the material inside these objects is also compositionally indistinguishable from the surrounding POZ material.

3.3.4 Fine-grained rims

Three of the 87 chondrules are contained within the clast and thus will be treated later (section 3.6). 81 (96%) of the remaining 84 chondrules are surrounded by fine-grained rims ranging in thickness from 5 to 160 μm. 39 (48%) of the 81 chondrules are entirely surrounded by rims (for example, Fig. 2a), whereas the remaining 42 chondrules (52%) partly lack rims (for example, Fig. 8a-e), among which 12 chondrules

Fig. 8

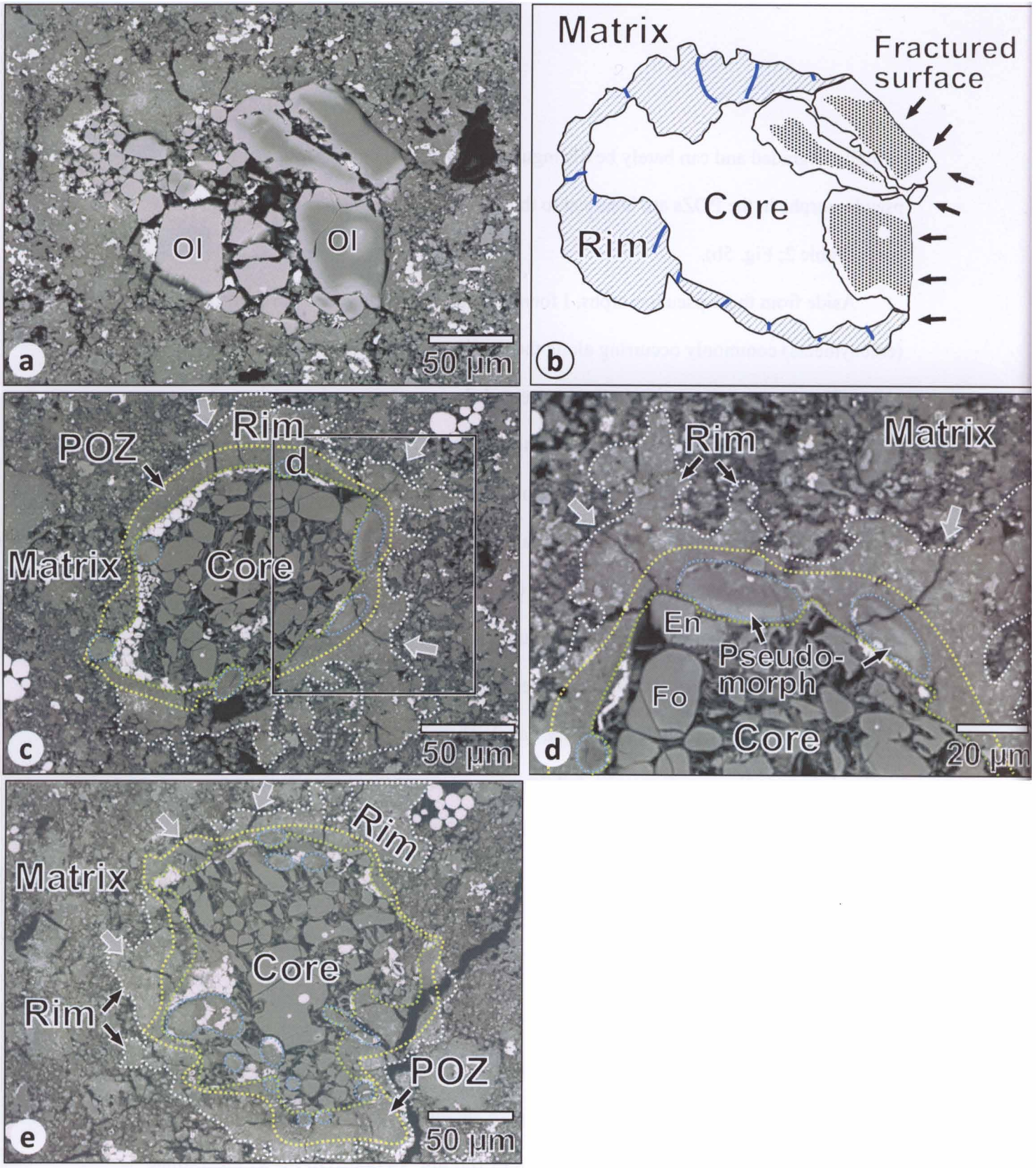

Fig. 8 (a) Back-scattered electron image of a type II chondrule that lacks a rim along its right side. Some of the olivine (Ol) phenocrysts exhibit Fe-Mg zoning. Note that the fractured surfaces of the zoned olivine phenocrysts are in direct contact with the matrix. (b) Illustration of (a) showing the chondrule core and rim. Fractures in the rim are indicated by dark blue lines. (c) Image of a chondrule, whose rim is partly lacking and exhibits a very irregular outline (white dotted line). Several pseudomorphs of opaque nodules (outlined by light blue dotted line) occur in the POZ. Fractures are indicated by gray arrows. (d) Image of boxed area f in (c) showing the core, POZ, rim, and matrix. Note that the rim/matrix boundary is very irregular. (e) Image of a chondrule, whose rim is partly lacking and exhibits a very irregular outline (white dotted line). Fractures are indicated by gray arrows. Fo=forsterite, En=enstatite, Mag=magnetite, Di=diopside, Phl=phyllosilicates.

lack rims along more than half of their circumferences. While chondrules and their rims are generally rounded, there are also abundant irregularly shaped ones. In addition, the rims are commonly disaggregated along the outer surfaces; thus, they exhibit very irregular outlines, and it is often difficult to determine the boundaries between the rims and the matrix (for example, Figs. 3c, 8c-e). These rims probably correspond to the non-layered rims or outer rims reported by Greshake et al. (2005); they are indeed similar in composition. Using TEM, these authors described the rims as consisting mainly of the same fine-grained phyllosilicates (saponite and serpentine) as those in the matrix.

The rims have a general resemblance in terms of porosity (Figs. 2d, 3d, 4b, c, and e) and chemical composition (Table 2; Fig. 5c) to the POZs, although they show differences in abundances of minor minerals and bulk Fe and Mg contents. The rims generally contain much higher total abundances of grains (<1–10 μm in diameter) of minor minerals than the POZs (7.3 versus 2.8 total vol.%; Table 1). The rims have higher abundances of Fe-Mg carbonate (4.3 versus 0.3 vol.% on average) and Fe-(Ni) sulfides (2.5 versus 0.4 vol.%) and lower abundances of magnetite (0.2 versus 2.0 vol.%) than the POZs (Table 1). Bulk compositions of the rims are significantly higher in Fe than those of the POZs (19.7 versus 17.4 wt. % as FeO on average; Table 2); this is probably the main reason for the rims to appear distinctly brighter than the POZs in the back-scattered electron images (see Figs. 2d, 3d, 4b, c, and e, for example). In the (Si+Al)–Fe–Mg ternary diagram (Fig. 5c), the rims show larger variations in both Fe and Mg contents than the POZs. This probably reflects the higher abundances of Fe-Mg carbonate and Fe-(Ni) sulfides in the rims.

The rims also have a generally similar chemical composition to the matrix (Table

2). However, they exhibit more significant differences in analytical totals (70.7 versus 57.1 wt.% on average; Table 2), texture, and abundances of the minor minerals, compared to the differences between the POZs and the rims. The rims have low porosity and smooth surfaces, whereas the matrix has abundant pores and a very uneven surface (Figs. 3c, 4b, 8d). Among the minor minerals, the abundances of carbonates are especially different (Table 1). Carbonates in the rims are exclusively Fe-Mg carbonate (4.3 vol.%), whereas the matrix contains both Fe-Mg carbonate (2.9 vol.%) and Ca carbonate (1.1 vol.%). The difference of Ca carbonate abundances is also evident in the combined X-ray elemental map (Fig. 9a and b). In addition, the rims contain much lower abundances of magnetite (0.2 versus 2.2 vol.%) and forsterite (0.3 versus 1.7 vol.%) than the matrix. In the (Si+Al)–Fe–Mg ternary diagram (Fig. 5d), analyses of the matrix plot on an area that is slightly more Mg-rich (~5 atm.% on average) and shows larger variations in Mg content than the rims. The distributions of the chemical analyses (Fig. 5d) are generally consistent with those obtained by Greshake et al. (2005) (Fig. 8 in their paper).

81 (96%) of the 84 chondrules contain fractures of 2–5 μm in width, most of which start radially from the chondrule core/POZ boundaries or the POZ/rim boundaries and terminate at the rim/matrix boundaries or within the rims (Figs. 4b, 8a-e). The presence of such fractures in the rims was also reported by Greshake et al. (2005). I ignored the fractures with thickness more than 10 μm since such thick fractures might be created during the preparation of the thin sections because of the extremely fragile nature of this meteorite.

Fig. 9

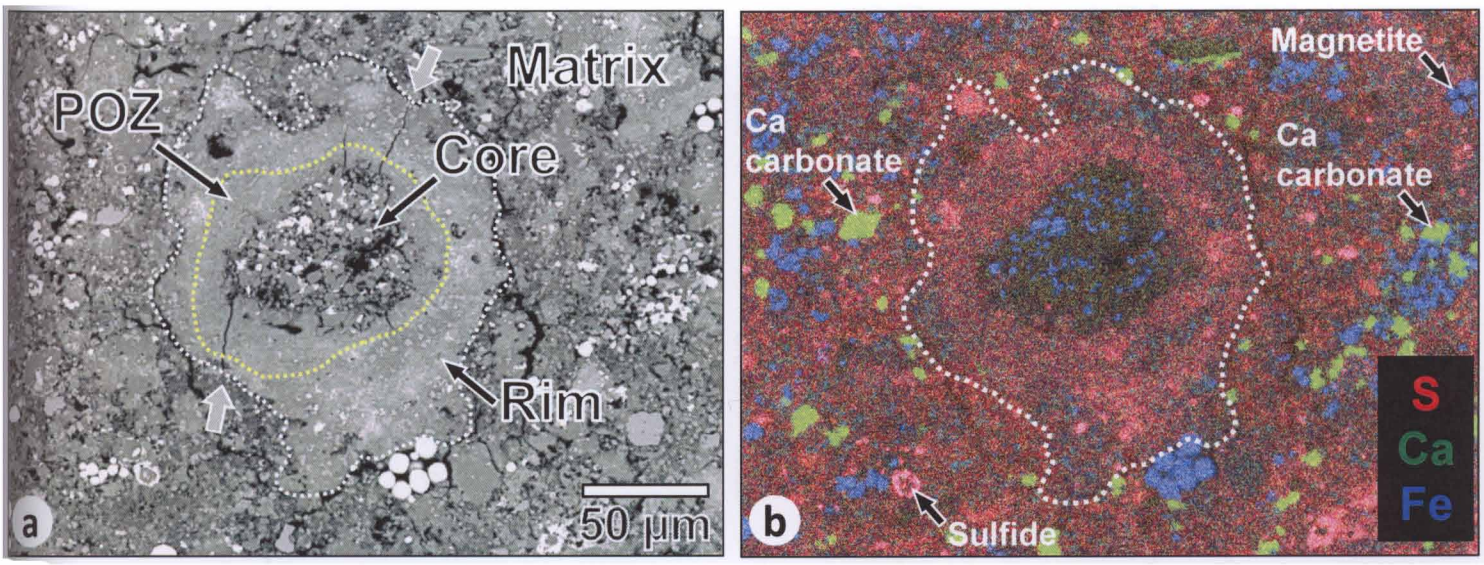

Fig. 9 (a) Back-scattered electron image of a chondrule core with a POZ and a rim. Fractures are indicated by gray arrows. (b) Combined X-ray elemental map of the area in (a) showing that Ca carbonate grains (green) are abundant in the matrix, whereas they are almost absent in the POZ and rim.

Table 3. EDS defocused beam analyses of phyllosilicates and pseudomorphs in chondrule cores and POZs (altered zones).

	Phyllosilicates replacing enstatite/mesostases		Pseudomorphs in chondrule cores		Pseudomorphs in POZS (altered zones)	
No. of chondrules	4		10		10	
No. of analyses	44		43		30	
		(s.d.)		(s.d.)		(s.d.)
Na_2O	0.17	0.12	0.12	0.11	0.14	0.10
MgO	19.3	3.8	18.6	2.1	18.8	2.5
Al_2O_3	4.04	1.70	4.50	1.46	4.60	1.79
SiO_2	31.8	6.2	33.8	3.3	34.3	4.1
P_2O_5	0.15	0.18	0.31	0.34	0.39	0.57
S	0.40	0.15	0.75	0.71	0.99	0.72
K_2O	0.19	0.96	0.08	0.04	0.06	0.04
CaO	0.51	0.59	0.42	0.16	0.45	0.18
TiO_2	0.09	0.09	0.12	0.08	0.16	0.09
Cr_2O_3	0.91	0.71	1.59	1.06	1.48	1.05
MnO	0.50	2.81	0.11	0.08	0.11	0.09
FeO	10.8	2.9	12.6	2.3	14.2	3.0
NiO	0.41	0.18	0.56	0.29	0.62	0.24
Total	69.3		73.6		76.3	

Table 2. WDS defocused beam analyses of POZs (altered zones), chondrule rims, matrices of clasts, and host matrix (wt.%).

	POZs (altered zones)		Rims		Matrices of clasts		Host matrix	
No. of chondrules/clasts	16		17		17			
No. of analyses	75		78		84		84	
		(s.d.)		(s.d.)		(s.d.)		(s.d.)
Na_2O	0.11	0.07	0.09	0.05	0.13	0.07	0.06	0.05
MgO	15.1	1.3	15.7	2.1	17.2	2.4	13.8	2.3
Al_2O_3	2.23	0.24	2.26	0.31	2.36	0.39	1.70	0.33
SiO_2	28.0	1.6	26.8	2.9	29.8	3.4	21.8	3.2
P_2O_5	0.26	0.10	0.23	0.10	0.25	0.07	0.15	0.08
S	2.73	0.76	3.12	1.59	2.40	1.34	2.67	1.09
K_2O	0.04	0.02	0.03	0.02	0.04	0.02	0.02	0.01
CaO	0.57	0.11	0.61	0.14	0.54	0.14	1.13	2.12
TiO_2	0.12	0.04	0.09	0.03	0.10	0.04	0.07	0.04
Cr_2O_3	0.58	0.34	0.44	0.15	0.38	0.09	0.33	0.10
MnO	0.13	0.05	0.14	0.09	0.12	0.08	0.16	0.10
FeO	17.4	1.8	19.7	3.8	17.6	3.1	13.8	2.6
NiO	1.64	0.32	1.47	0.38	1.45	0.55	1.38	0.46
Total	68.9		70.7		72.4		57.1	

3.4 CAIs

3.4.1 Cores

Both of the CAIs studied show evidence of intensive aqueous alteration. One of them (~500 μm in diameter) is composed of an interior consisting of Ca carbonate grains (3–20 μm in diameter), fine-grained Fe-poor spinel (<1.7% hercynite), and Mg-Al-rich phyllosilicates, rimmed by a 10–30 μm thick layer of spinel (Fig. 10a and b). The Mg-Al-rich phyllosilicates have compositions similar to those reported by Zolensky et al. (2002) from CAIs. The other CAI (~370 μm in diameter) has been more extensively altered and is composed mainly of Ca-Mg carbonate and Mg-Al-rich phyllosilicates, with minor relict grains (~1 μm) of spinel.

3.4.2 Fine-grained rims

Both CAIs are surrounded entirely by fine-grained rims 40–130 μm in thickness, which have texture, mineralogy, and chemical composition identical to those of the rims surrounding chondrules. However, they have neither pseudomorphs nor POZs such as those observed in the chondrules. Both CAIs also exhibit characteristic fractures of 2–5 μm in width, most of which start radially from the core/rim boundaries and terminate at the rim/matrix boundaries (Fig. 10a).

Fig. 10

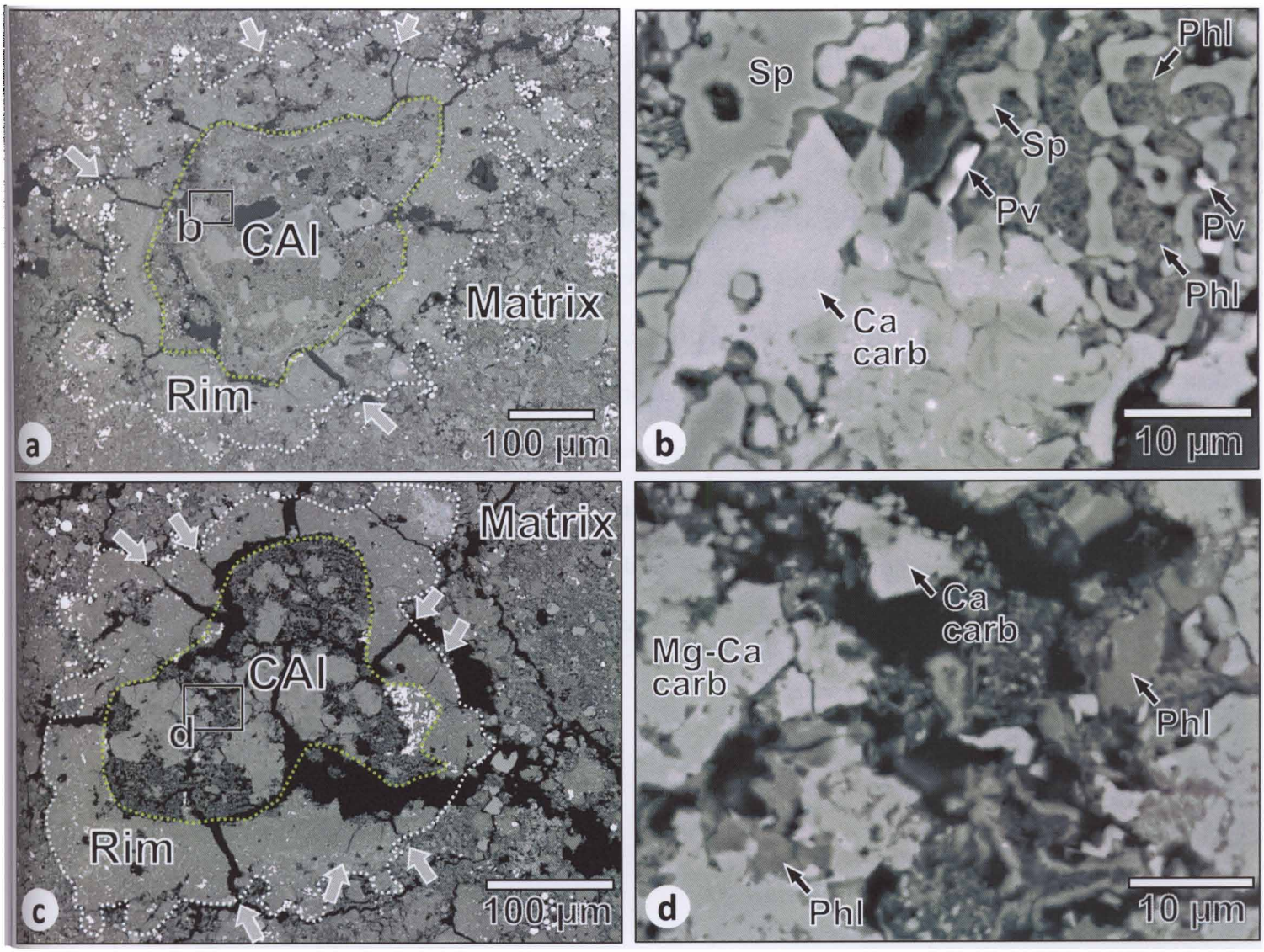

Fig. 10 (a) Back-scattered electron image of the larger CAI with a rim. The rim exhibits a very irregular outline (white dotted line). Some of the fractures in the rim are indicated by gray arrows. (b) Image of boxed area b in (a) showing that the interior of this CAI consists of spinel (Sp), phyllosilicates (Phl), Ca carbonate (Ca carb), and minor perovskite (Pv). (c) Back-scattered electron image of the other CAI. (d) Image of boxed area d in (c) showing the interior of this CAI consists of Mg-Ca carbonate (Mg-Ca carb), phyllosilicates (Phl), and Ca carbonate (Ca carb).

3.5 Forsterite-rich aggregates

3.5.1 Cores

I found 14 forsterite aggregates (2.1 vol.%) in the two thin sections. Their core sizes range from 50 to 660 μm in diameter with an average of 180 μm. Differ from chondrules, they have highly irregular shape, which made me distinguish them from chondrules. They are compact aggregates consisting of small grains (1–40 μm) of almost pure forsterite ($Fo_{>99.5}$). The intertspaces of forsterite grains are in most cases voids. In rare cases, small grains (<1–5 μm in diameter) of magnetite or spinel fill these interspaces. In contrast to the chondrules and CAIs, none of the 14 forsterite aggregates show evidence of aqueous alteration. They have neither pseudomorphs nor POZs (Fig. 11a–d).

3.5.2 Fine-grained rims

All of the forsterite aggregates except those three contained in the clast (Fig. 12a) are surrounded by fine-grained rims 5–160 μm in thickness, which are identical in texture, mineralogy, and chemical composition to the rims surrounding chondrules and CAIs. Some of the forsterite aggregates occur as clusters of separate aggregates embedded in rims (Fig. 11a and c). I consider the separate aggregates are actually parts of a single irregurlarly shaped aggregate.

The forsterite aggregate in Fig. 11b has a very irregularly shaped rim with variable thickness, and there is a tendency for the rim to be thick along the embayed regions of

Fig. 11

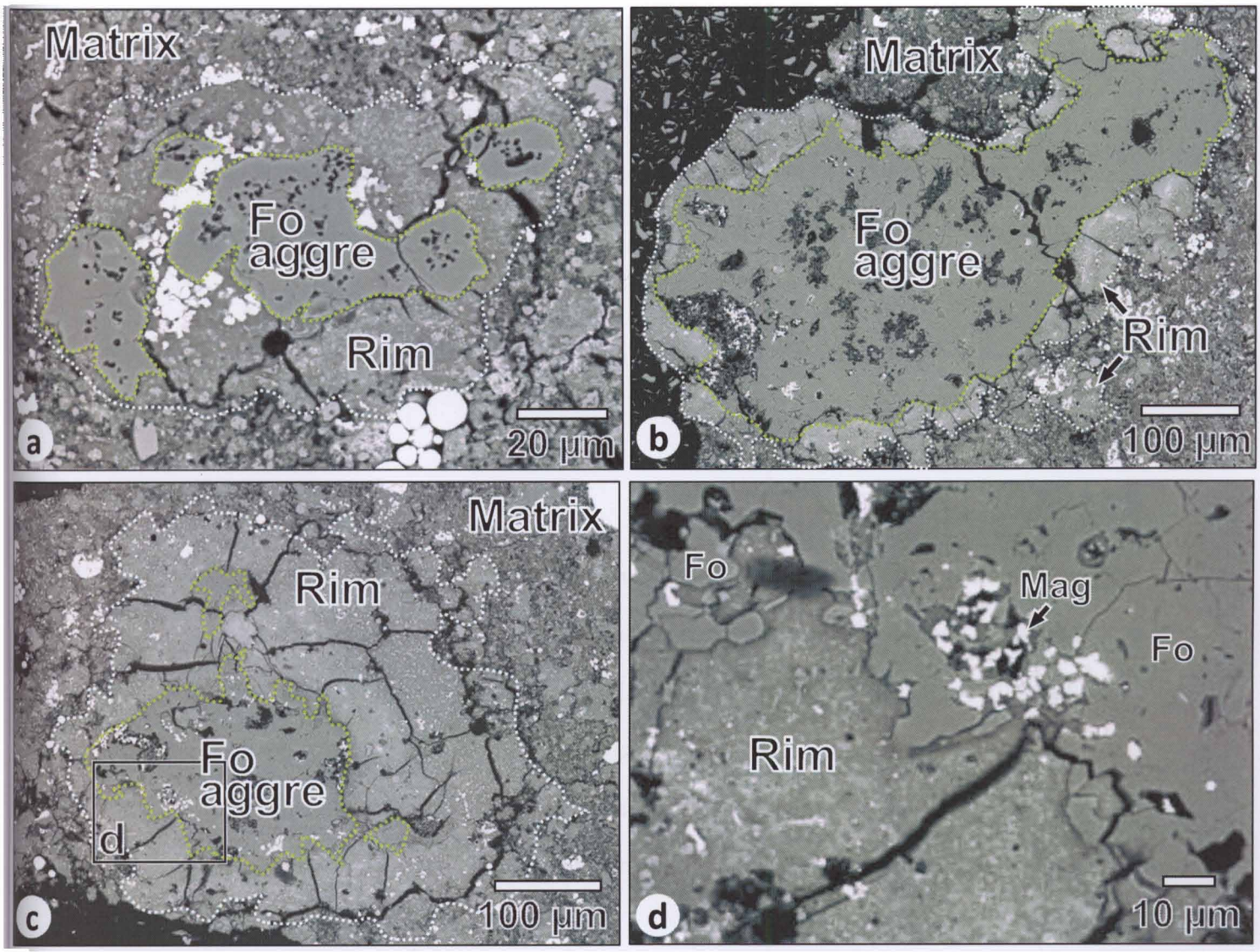

Fig. 11 (a) Back-scattered electron image of four forsterite aggregates (outlined by green dotted lines) surrounded by a rim. These four aggregates are considered to be parts of a single aggregate. Dark spots in the aggregate are pores. (b) Image of a large irregularly shaped forsterite aggregate with a rim. The rim also shows a very irregular outline and tends to be thick in the depressions of the aggregate surface. (c) Image of a forsterite aggregate with a thick rim having abundant fractures. Although there are two small aggregates near the main aggregate, we consider all the aggregates to be parts of a single aggregate. (d) Image of boxed area d in (c) showing that the forsterite aggregate is directly surrounded by the rim.

the aggregate surface.

Forsterite aggregates also exhibit exhibit characteristic fractures of 2–5 μm in width, most of which start radially from the core/rim boundaries and terminate at the rim/matrix boundaries (Figs. 11a–c).

3.6 Clasts

3.6.1 Matrix clasts

I found 55 lithic fragments (100–250 μm in diameter; 1.9 vol.%) that consist entirely of a fine-grained matrix material. The matrices of all these fragments are distinctly brighter in back-scattered electron images, less porous, and smoother on the surfaces than the host matrix (Fig. 1a–c). I consider all of these fragments to be clasts that were produced by brecciation. While relatively large clasts (>100 μm in diameter) generally exhibit round shapes (Fig. 1a), there are also abundant irregularly shaped clasts.

These matrix clasts have common mineralogical and textural characteristics (Fig. 1b) that are identical to those of the rims surrounding chondrules, CAIs, and forsterite aggregates. The average composition of the matrices of the clasts is also very similar to that of the rims (Table 2). In the (Si+Al)–Fe–Mg ternary diagram (Fig. 5e), the analyses of the matrices of the clasts plot on an area that almost completely overlaps with the analyses of the rims. In the combined X-ray elemental map (Fig. 13a and b), the difference in the distributions of Ca carbonate grains between the matrix of the clast and the host matrix is evident: Ca carbonate grains (green) are abundant in the matrix,

whereas they are almost absent in the clast. This distribution of Ca carbonate grains is similar to that in the chondrule/rim shown in Fig. 9b.

3.6.2 The largest clast

Figures 12 a–c show the largest clast (~450 μm in diameter) found from my sample that contains three chondrules and three forsterite aggregates. In the clast, as in the host meteorite, chondrules and aggregates larger than 50 μm in diameter were regarded as independent chondrules and aggregates. In distinguishing clasts from chondrules/rims on a cross section, there is a possibility that separate chondrules located close to each are actually parts of a single irregularly shaped chondrule. Therefore, I considered only the fragment containing both chondrules and forsterite aggregates, shown in Fig. 12, as a clast, since chondrules and forsterite aggregates are distinct components. The chondrules and forsterite aggregates in the clast have textures and mineralogy indistinguishable from those of the single chondrules and forsterite aggregates in the host meteorite. However, none of the chondrules and forsterite aggregates have rims; they are directly surrounded by the matrix of the clast.

The matrix of this large clast is distinctly brighter in back-scattered electron images, less porous, and smoother on the surface than the host matrix (Fig. 12a). The mineralogical and textural characteristics (Fig. 12c) are identical to those of the matrix clasts described above and those of the rims surrounding chondrules, CAIs, and forsterite aggregates. The only difference between the matrix of this clast and the matrix clasts is the presence of relatively large aggregates of framboidal magnetite in the left

Fig. 12

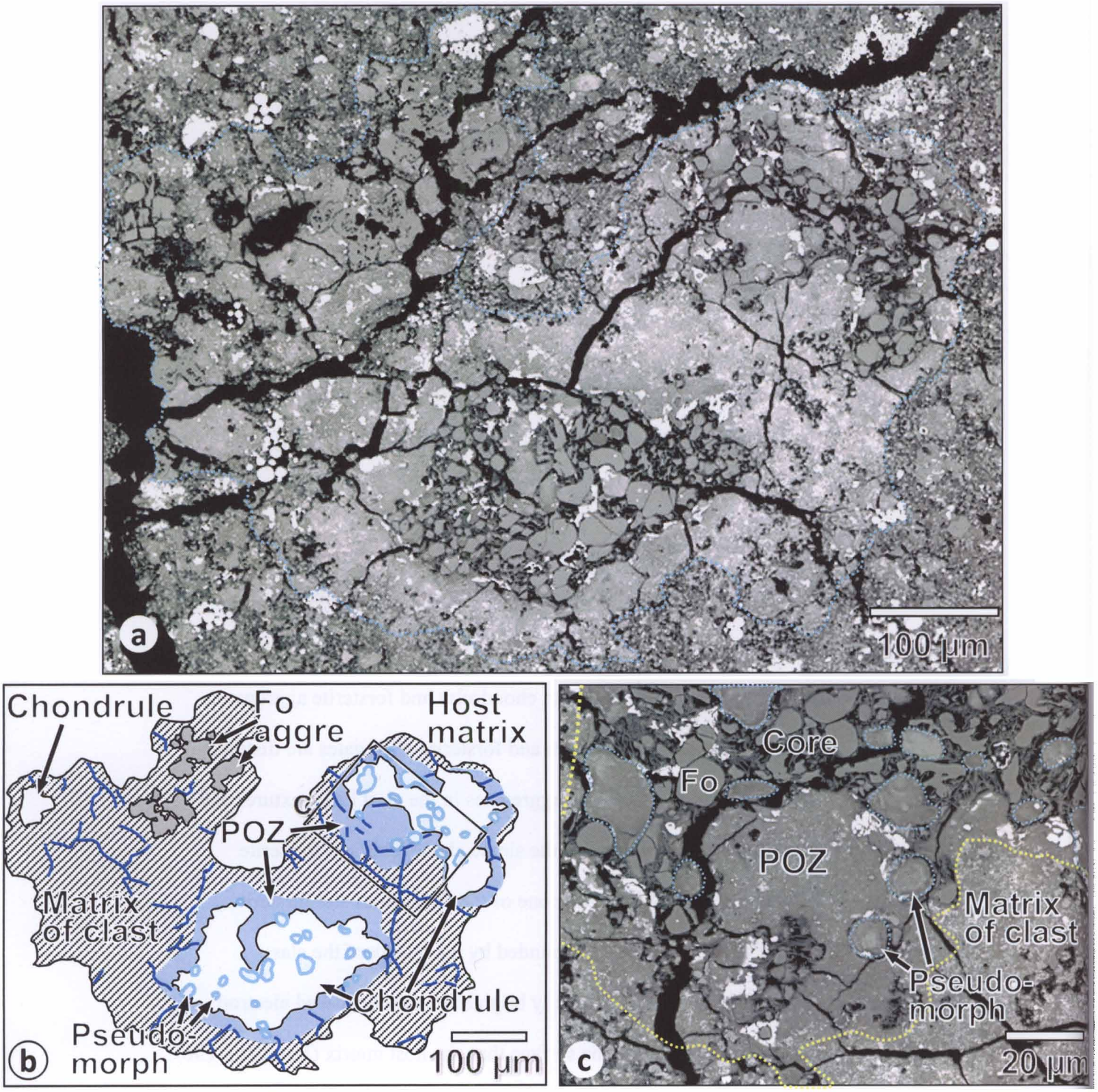

Fig. 12 (a) Back-scattered electron image of a clast (outlined by a light blue dotted line) containing three separate chondrules and three separate forsterite aggregates. (b) Illustration of (a). Pseudomorphs of opaque nodules in the chondrules are indicated by light blue lines. Fractures of 2–5 μm in width in the matrix of the clast are indicated by dark blue lines. (c) Image of boxed area c in (b) showing the chondrule core, POZ, and matrix of the clast. Pseudomorphs (outlined by light blue lines) occur in both the core and the POZ.

Fig. 13

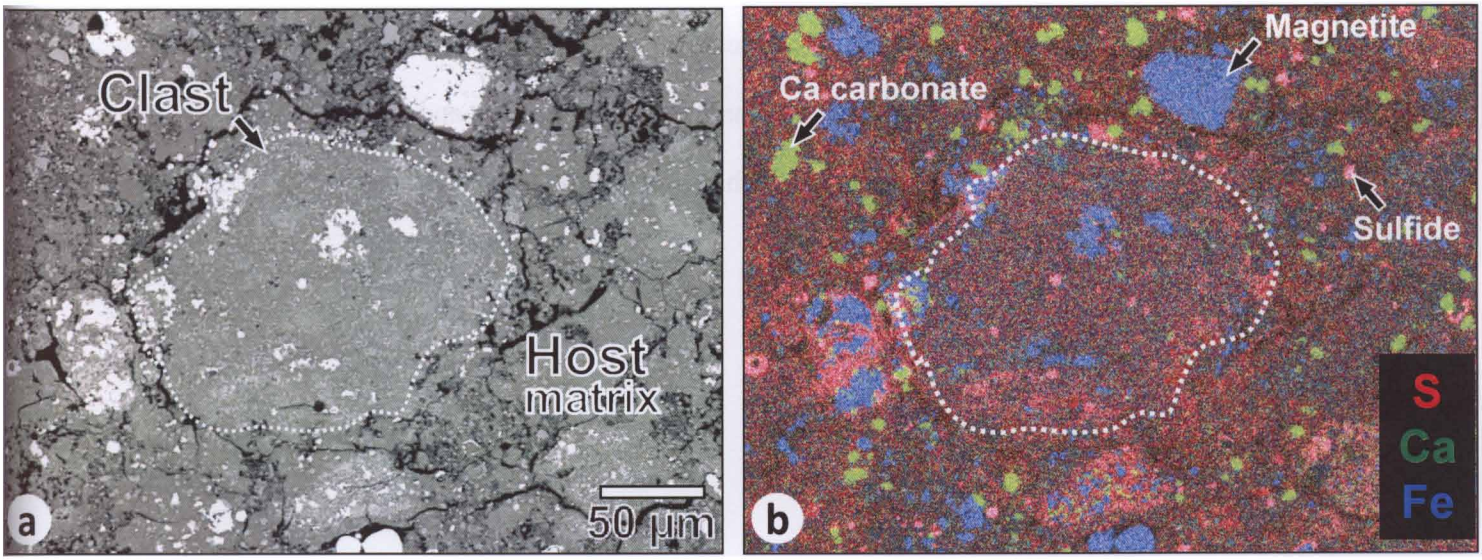

Fig. 13 (a) Back-scattered electron image of a matrix clast. (b) Combined X-ray elemental map of the area in (a) showing that Ca carbonate grains (green) are abundant in the matrix, whereas they are almost absent in the clast.

part of the matrix of this large clast. Such large framboidal magnetite is relatively rare in the matrix clasts (and the rims surrounding chondrules, CAIs and forsterite aggregates). The matrix of the clast exhibits relatively narrow fractures (2–5 μm in width) that run radially from the surfaces of the chondrules and forsterite aggregates and interconnect them (Fig. 12a and b). Most of these fractures terminate at the boundary between the clast and the host matrix. Wide fractures running through the clast and the host meteorite were probably formed during the handling process due to the extremely fragile nature of thie meteorite.

4.

DISCUSSION

4.1 Aqueously altered zones of chondrules

My microbeam chemical analyses indicate that the Mg-rich phyllosilicates, which were mostly formed by replacing enstatite and mesostases in the chondrules, can be identified as submicron-scale intergrowths of saponite and serpentine (Fig. 5a). The phyllosilicate-rich outer zones (POZs) of the chondrules are compositionally similar to these Mg-rich phyllosilicates, although the POZs show distinctly larger Fe contents (Fig. 5c), S, and Ni contents (by factors of approximately 7 and 4 for the latter two, respectively; Tables 2 and 3). These differences can be explained by the fact that the POZs contain higher abundances of fine grains of magnetite and Fe-(Ni) sulfides. I revealed that the POZs contain abundant pseudomorphs of opaque nodules that are identical to those inside the chondrule cores. From these results, I conclude that the POZs are altered zones that were formed by replacing enstatite and opaque nodules in the chondrule margins. Enstatite and opaque nodules are widely known to be less resistant to aqueous alteration than forsteritic olivine. Recently, Tomeoka and Ohnishi (2010) reported that the POP type chondrules in the Mokoia CV3 chondrite also have phyllosilicate-rich altered zones that were formed by replacing enstatite and opaque nodules in the chondrule peripheries (Figs. 2, 3, and 7 in their paper). Their textural characteristics are very similar to those observed in Tagish Lake.

I suggest that these altered zones were formed by the following processes. As aqueous alteration started and fluid reached the chondrules, mesostases, enstatite and opaque nodules in the chondrule margins were preferentially replaced by Mg-rich phyllosilicates. Fe, S, and Ni released from the opaque nodules were precipitated as fine grains of magnetite and Fe-(Ni) sulfide. Fe-Mg carbonate was also precipitated

simultaneously. As a result, the altered zones became enriched in Fe as well as S and Ni. The embayments along the chondrule surfaces (Figs. 2g-i, 6b) and the round objects (Figs. 2h, 7c) inside the altered zones had originally been opaque nodules, and they were later subjected to intensive aqueous alteration and exchange of atoms with the surrounding materials; as a result, their insides became indistinguishable from the outside; thus, they are actually remnants of pseudomorphs.

The POP type chondrules in Tagish Lake (69% of all the chondrules studied) have a tendency to have enstatite and opaque nodules in their peripheries, similar to those in Mokoia (Tomeoka and Ohnishi, 2010). Thus, I consider that many of the chondrules in Tagish Lake came to acquire altered zones along their peripheries. On the other hand, the CAIs and forsterite aggregates in Tagish Lake originally contained neither enstatite nor opaque nodules; thus, they did not form such altered zones. However, all of the CAIs and forsterite aggregates do have fine-grained rims that are common in texture, mineralogy, and chemical composition to the rims surrounding chondrules. These observations suggest that all of the rims have a common origin.

Then, an important question that arises from these considerations is whether the aqueous alteration of the chondrules and CAIs occurred under the present setting of the meteorite or not. I will return to this problem in section 4.3.

4.2 Evidence for chondrule-size scale brecciation and impacts

I found a clast that contains multiple chondrules and forsterite aggregates and numerous smaller matrix clasts, scattered throughout the matrix. Approximately half of

the chondrules partly or entirely lack rims, and the rims are commonly disaggregated along their outer surfaces and exhibit very irregular outlines. These observations suggest that extensive brecciation occurred on chondrule-size scales (<1 mm) in the carbonate-poor lithology of the Tagish Lake parent body. I think that it is reasonable to assume that the brecciation was basically driven by impacts on the parent body.

The rims surrounding chondrules, CAIs, and forsterite aggregates contain characteristic fractures (Figs. 4b, 8a and d, 10a, and 11c). Greshake et al. (2005) suggested that such fractures in the rims were formed as a result of volume expansion during oxidation of metal to magnetite in opaque nodules, as previously interpreted for the fayalite-hedenbergite-magnetite filling veins in the rims in the MAC88197 chondrite (Krot et al., 2000). However, in the case of Tagish Lake, the fractures are not filled by any minerals, and the rims surrounding CAIs and forsterite-rich aggregates, both of which contain no opaque nodules, do have fractures in the same abundance as in the rims around chondrules (Figs. 10a and 11c).

Fractures are also reported to be common in the phyllosilicate-rich rims and clasts in the Vigarano CV3 chondrite (Tomeoka and Tanimura, 2000). These authors suggested that the fractures had been formed during impact processes that had occurred before the chondrules and their rims were incorporated into the place where the meteorite finally lithified. They thought that the porous matrix composed of fine-grained, fluffy hydrous phyllosilicates is mechanically weak, so that it tends to be easily fractured when impacted (also see Tomeoka et al. (2003) and Tomeoka and Ohnishi (2010) for this interpretation). I suggest that the fractures in the rims of chondrules, CAIs, and forsterite aggregates in Tagish Lake were also formed by impacts in a location (or locations) on the meteorite parent body.

4.3 Relationship between chondrules, rims, and matrix: setting of aqueous alteration

The altered zones of chondrules and their surrounding rims are similar in that they are low in porosity and have smooth surfaces, although they exhibit some differences in abundances of minor minerals and chemical compositions as described in section 3.4. The boundaries between the altered zones and the rims are commonly irregular and not clearly discernible. There are abundant fractures that start from the altered zones and run through the rims. These observations suggest that the altered zones and the rims had been next to each other and had experienced aqueous alterationbefore formation of the fractures. In comparison, the rims and the host matrix exhibit more significant differences in texture, abundances of minor minerals, and chemical composition as also already described in section 3.4. These differences suggest that the rims and the matrix experienced aqueous alteration under distinct conditions.

In contrast to the chondrules and forsterite aggregates in the host meteorite, those contained in the clast (Fig. 12a and b) have no rims and are directly surrounded by the matrix of the clast. The matrix of the clast and the other numerous matrix clasts are identical in texture, mineralogy, and chemical composition to the rims surrounding chondrules, CAIs, and forsterite aggregates. All of these results suggest that the clasts and the rims have a common origin.

From these observations and considerations, I suggest that the chondrules, CAIs, forsterite aggregates, and their rims (hereafter generically referred to as chondrules/rims) and the clasts originated from a common precursor region in the meteorite parent body that was different from the location where the host meteorite was

finally lithified. That is, the chondrules/rims are actually clasts that were produced by brecciation after aqueous alteration in the precursor region. Subsequently, they were transported in the parent body and finally incorporated to the present host matrix. This means that the rims are remnants of matrix material that filled the interspaces among the chondrules, CAIs, and forsterite aggregates in the precursor material. As mentioned above, the fine-grained, porous, hydrous matrix tends to be preferentially fragmented upon impacts. During brecciation and transportation, many of the chondrules probably lost their rims, and numerous small matrix clasts were generated simultaneously. This model is essentially consistent with that proposed by Nakamura et al. (2003) for the Tagish Lake carbonate-rich lithology. One difference from their model is the timing of the formation of Fe-Mg carbonate; they stated that the formation of Mg-Fe carbonate postdates the final accretion of the clasts onto the host matrix of the carbonate-rich lithology since they observed Mg-Fe carbonate on the surface of the clasts. However, in the carbonate-poor lithology, I did not observe any evidence for post-accretionary aqueous alteraion such as veins filling fractures and Fe-Mg carbonates precipitated at the interface of rims (clasts) and host matrix. Some degree of interaction between rims (clasts) and host matrix could occur after the clasts were re-incorporated to host matrix because of the residual heat of clasts or parent body, resulting in ambiguous boundary between clasts and host matrix.

4.4 Precursor lithology of the chondrules/rims and clasts

With regard to the precursor lithology of the chondrules/rims and clasts, the

occurrence of carbonates may provide insight. Carbonates are known to be among the typical products of aqueous alteration. The carbonates occurring in the rims and the matrix of the clasts are exclusively Fe-Mg carbonate, whereas the host matrix (in the carbonate-poor lithology) contains Fe-Mg carbonate and Ca carbonate. On the other hand, the carbonate-rich lithology in Tagish Lake is characterized by a high abundance of Fe-Mg carbonate and a very low abundance of Ca carbonate (Zolensky et al., 2002; Nakamura et al., 2003). Therefore, my results suggest that the precursor lithology of the chondrules/rims and clasts in my sample, if any, are genetically related to the carbonate-rich lithology rather than their host carbonate-poor lithology, although the abundance of Fe-Mg carbonate is much lower in the former than the latter. Thus, these further imply that the precursor lithology of the chondrules/rims and clasts in my sample is distinct from both carbonate-poor and carbonate-rich lithologies.

4.5 Formation model

From the results and the above consideration, I propose a model for the formation of the carbonate-poor lithology in Tagish Lake (Fig. 14). Originally, chondrules, CAIs, and forsterite aggregates were embedded in a matrix in a region of the meteorite parent body. I assume that the matrix was initially anhydrous (stage 1). Due to the introduction of an aqueous fluid, aqueous alteration started, and the fine-grained, porous matrix was preferentially replaced by phyllosilicates. Simultaneously, Fe-Mg carbonates were precipitated in the matrix. In chondrules, enstatite and opaque nodules in their margins were preferentially replaced by phyllosilicates, thus forming altered zones. Opaque

Fig. 14

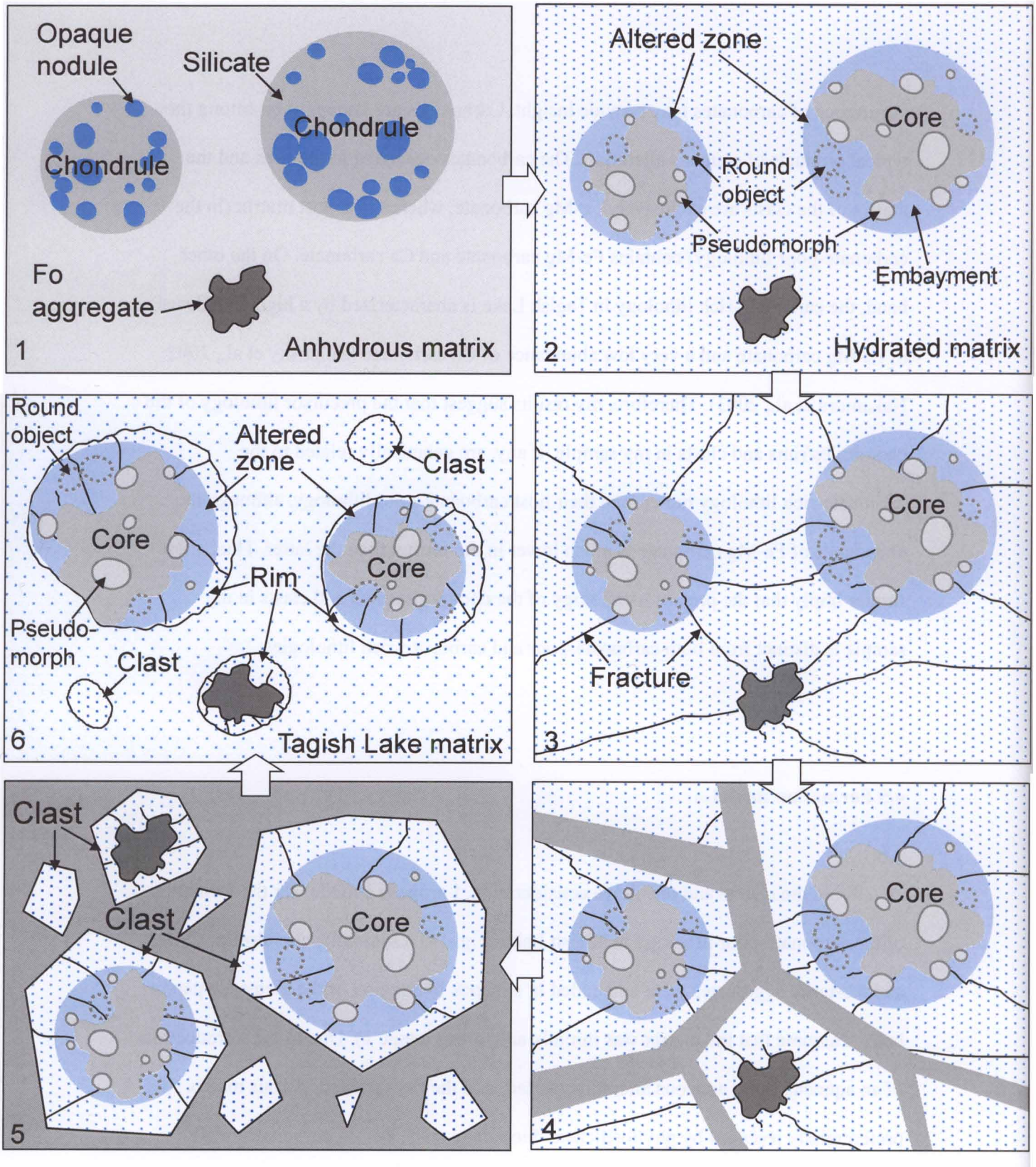

Fig. 14 Model for the formation of the carbonate-poor lithology of Tagish Lake. It was formed by a six-stage process: (1) chondrules and forsterite aggregates embedded in an anhydrous matrix at a location of the meteorite parent body; (2) aqueous alteration at this location; (3) fracture formation in the altered zones of chondrules and matrix due to impacts; (4) preferential fragmentation of the matrix due to multiple and/or stronger impacts; (5) ejection of chondrule/rim and aggregate/rim clasts and matrix clasts; and (6) abrasion of the clasts during transportation and incorporation of the clasts into the present Tagish Lake matrix (see text for details).

nodules inside chondrules were altered to pseudomorphs. Framboidal magnetite was probably also formed by replacing opaque nodules in this stage (stage 2). After the aqueous alteration ceased, probably due to the exhaustion of the fluid, this region was impacted, and fractures were formed preferentially in the altered zones and matrix (stage 3). As a result of multiple and/or stronger impacts, the matrix was preferentially broken, and individual chondrules were ejected as clasts, with their surrounding matrix attached to their peripheries. The matrix was also fragmented to small clasts (stage 4). These clasts were abraded during brecciation and transportation on the surface (or in the interior) of the parent body, resulting in the formation of chondrules/rims and clasts. At this stage, many of the chondrules/rims partly or entirely lost their rims (stage 5). The chondrules/rims and clasts were finally mixed with the present host matrix and lithified to the carbonate-poor lithology (stage 6).

4.6 Comparison to other chondrites

My model is essentially consistent with those proposed by Tomeoka and Tanimura (2000) and Tomeoka and Ohnishi (2010) for the hydrated chondrules/rims in the Vigarano and Mokoia CV3 chondrites, respectively. It is probably also consistent with the model proposed by Jogo et al. (2009) for the four unusual oxidized CV (CV_{oxd}) clasts in Vigarano. The rims in Vigarano have fractures like those in Tagish Lake, whereas the rims in Mokoia and the matrices of the CV_{oxd} clasts in Vigarano have no fractures but instead veins filled with Fe-rich olivine, magnetite, and Fe-(Ni) sulfides. The differences of formation processes between these three objects can be interpreted as

follows. Fracture formation due to impacts in the precursor lithology of the Vigarano rims occurred after water was exhausted, as in the case of Tagish Lake. On the other hand, in the precursor lithologies of the Mokoia rims and the Vigarano CV_{oxd} clasts, aqueous activity still continued when the fractures were formed, thus forming the fracture-filling veins.

On the other hand, in the CM chondrites, chondrules and their fine-grained rims have significantly different texture, mineralogy and chemical compositions from those of Tagish Lake (cf. Metzler et al., 1992), which indicates that the alteration conditions and/or precursor mineralogy of them were quite different. In addition, most of the CM chondrites are theirselves breccias, thus it is difficult to distinguish which texture is original and which is not, especially regarding fractures in rims. Primary accretionary rocks, which consist solely of chondrules (or CAIs, PCPs and so on) plus their rims, can be regarded as the aggregate of chondrules/rim clasts.

In the Vigarano and Mokoia meteorites, the rims are intensively hydrated, while the host matrices are largely anhydrous; this implies that their parent body (or bodies) had a heterogeneous distribution of water and various degrees of aqueous alteration occurred in different regions. On the other hand, in the Tagish Lake meteorite, both the rims and the host matrix are intensively hydrated; this implies that the Tagish Lake parent body had a homogeneous distribution of water and that a high degree of aqueous alteration occurred throughout the parent body. However, even in this case, the conditions of aqueous alteration were evidently not uniform. A recent study by Izawa et al. (2010) reported two new distinct lithologies from Tagish Lake, in addition to the carbonate-rich and -poor lithologies. My study also revealed that the precursor lithology of the chondrules/rims and clasts in my sample appear to be distinct from both the

carbonate-rich and -poor lithologies, as discussed above (section 4.4). These results imply that the conditions for aqueous alteration varied considerably on the Tagish Lake parent body.

All of these results and considerations, taken together, suggest that the Vigarano, Mokoia, and Tagish Lake meteorites are common in that the hydrated chondrules/rims and clasts were transported from a location (or locations) in their parent bodies different from where the host meteorites finally existed. Therefore, I suggest that the series of parent-body processes that I propose here for the formation of Tagish Lake is not unique to this meteorite but is common to many other chondrites.

5.

CONCLUSIONS

(1) Most of the 87 chondrules in the Tagish Lake meteorite studied contain many pseudomorphs of opaque nodules consisting mainly of phyllosilicates (saponite and serpentine) and minor amounts of magnetite and Fe-(Ni) sulfides. The magnetite commonly occurs as framboidal aggregates. Most of the porphyritic olivine-pyroxene chondrules have altered zones that were formed by replacing enstatite and opaque nodules along the peripheries.

(2) Most of the chondrules and all of the CAIs and forsterite aggregates studied are surrounded entirely or partly by fine-grained rims. The rims are commonly disaggregated along the outer surfaces and exhibit very irregular outlines. Many of the rims contain crosscutting fractures that start from the inner altered zones. The rims and the altered zones are similar in chemical composition and texture, although they exhibit differences in abundances of minor minerals. These observations suggest that the rims and their enclosing objects experienced aqueous alteration simultaneously before acquiring the fractures.

(3) The rims and the matrix show more significant differences. The rims are distinctly richer in Fe and less porous than the matrix. The rims contain abundant Fe-Mg carbonate but no Ca carbonate, whereas the matrix contains both carbonates. The rims contain much lower abundances of magnetite and higher abundances of Fe-(Ni) sulfides. These observations suggest that the rims and the matrix experienced aqueous alteration under distinct conditions.

(4) I found a clast containing multiple chondrules and forsterite aggregates and numerous smaller matrix clasts. The chondrules and forsterite aggregates in the clasts have no rims, and the matrices of the clasts are mineralogically and texturally identical to the rims. These observations suggest that the chondrules/rims and the clasts

constituted a common precursor material and that brecciation on submillimeter scales occurred extensively in the precursor region of the parent body.

(5) I suggest that the chondrules/rims and the clasts originated from a common precursor region in the meteorite parent body that was different from the location where the host meteorite was finally lithified. The chondrules/rims are actually clasts that were produced by brecciation after aqueous alteration in the precursor region. They were subsequently transported in the parent body and finally incorporated into the present host matrix. These processes are consistent with the models proposed for the carbonate-rich lithology of Tagish Lake (Nakamura et al., 2003) and the hydrated chondrules/rims in the Vigarano and Mokoia CV3 chondrites (Tomeoka and Tanimura, 2000; Tomeoka and Ohnishi, 2010). From these results, I suggest that similar parent-body processes occurred in many other chondrites.

ACKNOWLEDGEMENT

I greatly thank Professor K. Tomeoka for his guidance and encouragement in every stage of this study. I also thank Dr. M. E. Zolensky for the Tagish Lake sample, and Drs. N. Tomioka, Y. Seto, and all other current and past members of the Planetary Material Science Laboratory at Kobe University for technical supports and helpful discussions. I also greatly thank my parents, sister, and grand parents for their encouragements and supports. Electron microprobe analysis was performed at the Instrumentation Analysis Division in the Center for Supports to Research and Education Activities, Kobe University.

REFERENCES

Bland P. A., Cressey G. and Menzies O. N. (2004) Modal mineralogy of carbonaceous chondrites by X-ray diffraction and Mössbauer spectroscopy. *Meteorit. Planet.Sci.* 39, 3–16.

Blinova A. and Herd C. D. K. (2010) Insights into the mineralogy of the Tagish Lake meteorite through EPMA, XRD and CL. *Lunar Planet. Sci.* XXXXI Lunar Planet. Inst., Houston. #2140 (abstr.).

Brown P. G., Hildebrand A. R., Zolensky M. E., Grady M., Clayton R. N., Mayeda T. K., Tagliaferri E., Spalding R., MacRae N. D., Hoffman E. L., Mittlefehldt D. W., Wacker J. F., Bird J. A., Campbell M. D., Carpenter R., Gingerich H., Glatiotis M., Greiner E., Mazur M. J., McCausland P. JA., Plotkin H., Rubak Mazur T. (2000) The fall, recovery, orbit, and composition of the Tagish Lake meteorite: A new type of carbonaceous chondrite. *Science* 290, 320–325.

Clayton R. N. and Mayeda T. K. (2001) Oxygen isotopic composition of the Tagish Lake carbonaceous chondrite. *Lunar Planet. Sci. XXXII* Lunar Planet. Inst., Houston. #1885 (abstr.).

Cuzzi J. N., Ciesla F. J., Petaev M. I., Krot A. N., Scott E. R. D. and Weidenschilling S. J. (2005) Nebula evolution of thermally processed solids: reconciling models and meteorites. In *Chondrites and the Protoplanetary Disk* (eds. A. N. Krot, E. R. D. Scott and B. Reipurth) Astron. Soc. Pac. Conf. Ser., pp. 732–773.

Friedrich J. M., Wang M., and Lipschutz M. E. (2002) Comparison of the trace element composition of Tagish Lake with other primitive carbonaceous chondrites. *Meteorit. Planet. Sci.* 37, 677–686.

Fuchs L. H. and Olsen E. (1973) Composition of metal in type III carbonaceous chondrites and its relevance to the source-assignment of lunar metal. *Earth Planet. Sci. Lett.* 18, 379–384.

Grady M. M., Verchovsky A. B., Franchi I. A., Wright I. P. and Pillinger C. T. (2002) Light element geochemistry of the Tagish Lake CI2 chondrite: comparison with CI1 and CM2 meteorites. *Meteorit. Planet. Sci.* 37, 713–735.

Greshake A., Krot A. N., Flynn G. J. and Keil K. (2005) Fine-grained dust rims in the Tagish Lake carbonaceous chondrite: Evidence for parent body alteration. *Meteorit. Planet. Sci.* 40, 1413–1431.

Izawa M. R. M., Flemming R. L., King P. L., Peterson R. C. and McCausland P. J. A. (2010) Mineralogical and spectroscopic investigation of the Tagish Lake carbonaceous chondrite by X-ray diffraction and infrared reflectance spectroscopy. *Meteorit. Planet. Sci.* 45, 675–698.

Jogo K., Nakamura T., Noguchi T. and Zolotov M. Y. (2009) Fayalite in the Vigarano CV3 carbonaceous chondrite: Occurrences, formation age and conditions. *Earth Planet. Sci. Lett.* 287, 320–328.

Keller L. P. and Flynn G. J. (2001) Matrix mineralogy of the Tagish Lake carbonaceous chondrite: TEM and FTIR studies. *Lunar Planet. Sci. XXXII* Lunar Planet. Inst., Houston. #1639 (abstr.).

Kimura M., Grossman J. N. and Weisberg M. K.. (2008) Fe-Ni metal in primitive chondrites: Indicators of classification and metamorphic conditions for ordinary and CO chondrites. *Meteorit. Planet. Sci.* 43, 1161–1177.

Krot A. N., Brearley A. J., Petaev M. I., Kallemeyn G. W., Sears D. W. G., Benoit P. H., Hutcheon I. D., Zolensky M. E. and Keil K. (2000) Evidence for low-temperature

growth of fayalite and hedenbergite in MacAlpine Hills 88107, an ungrouped carbonaceous chondrite related to the CM-CO clan. *Meteorit. Planet. Sci.* 35, 1365–1386.

Metzler K., Bischoff A. and Stöffler D. (1992) Accretionary dust mantles in CM chondrites: Evidence for solar nebula processes. *Geochim. Cosmochim. Acta* 56, 2873–2897.

Mittlefehldt D. W. (2002) Geochemistry of the ungrouped carbonaceous chondrite Tagish Lake, the anomalous CM chondrite Bells, and comparison with CI and CM chondrites. *Meteorit. Planet. Sci.* 37, 703–712.

Nakamura T., Noguchi T., Zolensky M. E., Tanaka M. (2003) Mineralogy and noble-gas signatures of the carbonate-rich lithology of the Tagish Lake carbonaceous chondrite: evidence for an accretionary breccia. *Earth Planet. Sci. Lett.* 207, 83–101.

Noguchi T., Nakamura T. and Nozaki W. (2002) Mineralogy of phyllosilicate-rich micrometeorites and comparison with Tagish Lake and Sayama meteorites. *Earth Planet. Sci. Lett.* 202, 229–246.

Russell S. D. J., Longstaffe F.J., King P. L. and Larson T. E. (2010) The oxygen-isotope composition of chondrules and isolated forsterite and olivine grains from the Tagish Lake carbonaceous chondrite. *Geochim. Cosmochim. Acta* 74, 2484–2499.

Sears D. W. G., Benoit P. H. and Jie L. (1993) Two chondrule groups each with distinctive rims in Murchison recognized by cathodoluminescence. *Meteoritics* 28, 669–675.

Simon S. B. and Grossman L. (2003) Petrography and mineral chemistry of the anhydrous component of the Tagish Lake carbonaceous chondrite. *Meteorit.*

Planet. Sci. 38, 813–825.

Tomeoka K. and Ohnishi I. (2011) A hydrated clast in the Mokoia CV3 carbonaceous chondrite: Evidence for intensive aqueous alteration in the CV parent body. *Geochim. Cosmochim. Acta 75*, 6064–6079.

Tomeoka K. and Ohnishi I. (2010) Indicators of parent-body processes: Hydrated chondrules and fine-grained rims in the Mokoia CV3 carbonaceous chondrite. *Geochim. Cosmochim. Acta 74*, 4438–4453.

Tomeoka K. and Tanimura I. (2000) Phyllosilicate-rich chondrule rims in the Vigarano CV3 chondrite: Evidence for parent-body processes. *Geochim. Cosmochim. Acta* 64, 1971–1988.

Tomeoka K., Kiriyama K., Nakamura K., Yamahana Y., and Sekine T. (2003) Interplanetary dust from the explosive dispersal of hydrated asteroids by impacts. *Nature* 423, 60–62.

Trigo-Rodriguez J. M., Rubin A. E. and Wasson J. T. (2006) Non-nebular origin of dark mantles around chondrules and inclusions in CM chondrites. *Geochim. Cosmochim. Acta* 70, 1271–1290.

Zolensky M. E., Nakamura K., Gounelle M., Mikouchi T.; Kasama T., Tachikawa O. and Tonui E. (2002) Mineralogy of Tagish Lake: An ungrouped type 2 carbonaceous chondrite. *Meteorit. Planet. Sci.* 37, 737–761.